AD_____

Award Number: DAMD17-99-1-9250

TITLE: Expression Profiling of Tyrosine Kinase Genes

PRINCIPAL INVESTIGATOR: Heinz Ulrich Weier, Ph.D.

CONTRACTING ORGANIZATION: University of California at Berkeley
Berkeley, California 94720

REPORT DATE: August 2000

TYPE OF REPORT: Annual

PREPARED FOR: U.S. Army Medical Research and Materiel Command
Fort Detrick, Maryland 21702-5012

REPORT DOCUMENTATION PAGE

Form Approved
OMB No. 074-0188

1. AGENCY USE ONLY (Leave blank)	2. REPORT DATE	3. REPORT TYPE AND DATES COVERED
	August 2000	Annual (1 Aug 99 - 31 Jul 00)

4. TITLE AND SUBTITLE
Expression Profiling of Tyrosine Kinase Genes

5. FUNDING NUMBERS
DAMD17-99-1-9250

6. AUTHOR(S)
Heinz Ulrich Weier, Ph.D.

7. PERFORMING ORGANIZATION NAME(S) AND ADDRESS(ES)
University of California at Berkeley
Berkeley, California 94720

E-MAIL:
UGWeier@lbl.gov

8. PERFORMING ORGANIZATION REPORT NUMBER

9. SPONSORING / MONITORING AGENCY NAME(S) AND ADDRESS(ES)
U.S. Army Medical Research and Materiel Command
Fort Detrick, Maryland 21702-5012

10. SPONSORING / MONITORING AGENCY REPORT NUMBER

11. SUPPLEMENTARY NOTES
This report contains colored photos

12a. DISTRIBUTION / AVAILABILITY STATEMENT
Approved for public release; distribution unlimited

12b. DISTRIBUTION CODE

13. ABSTRACT ***(Maximum 200 Words)***

There is strong evidence that the expression of genes involved in signal transduction such as protein kinases is altered in tumor cells and that the aberrant expression of one or several of these genes parallels the progression of tumors to a more malignant phenotype. We developed a DNA micro-array based screening system to monitor the level of expression of tyrosine kinase (tk) genes and to derive quantitative information to support prognostication and therapeutic decisions. In the first year of this effort, we finished the development and testing of hardware necessary to prepare the DNA micro-arrays, performed RNA extraction, cDNA preparation and labelling reactions, and defined a working protocol for array hybridization and quantitative analysis. Our prototye design simultaneously measures the expression of 58 different tk genes. Additional targets for investigation will be defined by the ongoing molecular cloning and sequencing of gene transcripts found in breast cancer cell lines and clinical specimens. Using a set of phenotypically well characterized breast cancer cell lines, the system has proven to be able to deliver reproducible data regarding changes in tk gene expression during cell transformation and progression towards a more malignant phenotype.

14. SUBJECT TERMS	15. NUMBER OF PAGES
Breast Cancer, gene expression, tyrosine kinase	37
	16. PRICE CODE

17. SECURITY CLASSIFICATION OF REPORT	18. SECURITY CLASSIFICATION OF THIS PAGE	19. SECURITY CLASSIFICATION OF ABSTRACT	20. LIMITATION OF ABSTRACT
Unclassified	Unclassified	Unclassified	Unlimited

NSN 7540-01-280-5500

Standard Form 298 (Rev. 2-89)
Prescribed by ANSI Std. Z39-18
298-102

Table of Contents

INTRODUCTION:

Tumor development is typically accompanied by changes in the way cells interact with their environment, and how signals are transduced from the cell membrane to the cell nucleus. Among the hundreds of genes involved in signal transduction and the cellular response to external stimuli, only few genes have yet been identified as being aberrantly expressed in breast cancer and their expression pattern could be related to tumor growth.

Aberrant expression of various receptor or cytosolic tyrosine kinase genes and their hyperexpression, in particular, are common phenomena in breast cancer, where this is believed to alter cell growth and response to external signals such as growth factors, hormones etc. Knowledge about the level of expression of many tyrosine kinase genes at the same time would contribute significantly to a better understanding of the processes of oncogenesis and tumor progression. However, many presently used techniques measure the expression of only one or two genes. Thus, they are likely to miss an important correlation between the spatial or temporal expression of several genes and tumor stage, its chances to progress to a more malignant invasive phenotype or the chances of metastasis and recurrence.

The present project targets development of a novel assay format that allows to determine the level of expression of many different genes. Our rapid assay will use innovative DNA micro-arrays carrying small amounts of individual tyrosine kinase gene-specific targets to simultaneously determine the expression level of up to 100 tyrosine kinase genes using a small number of cells. Three years of research and development will lead to a set of gene-specific markers to describe breast cancer progression and a simple device capable of performing inexpensive expression profiling of these markers.

Research and development efforts in the first year of this 3-year project focussed on the design and test of robotic instruments to prepare the DNA micro-arrays, the preparation of prototype arrays carrying a pre-existing set of tyrosine kinase gene fragments to optimize hybridization and detection protocols as well as the molecular cloning and sequencing of breast cancer-specific tyrosine kinase gene transcripts.

BODY:

To extend our pre-existing panel of tyrosine kinase genes and to identify tyrosine kinase (tk) genes expressed in normal and neoplastic breast tissues, we prepared cDNAs from eleven cell lines including the six commonly available established cell lines ZR7S, SKBR3, BT474(2 different cultures), BT468, BT549, and MCF-7(2 different cultures). The cDNA's were prepared by reverse transcription using an oligo-(dT) primer and a commercial kit (Promega Inc.). Furthermore, RNA isolated from five phenotypically well characterized cell lines was provided by Dr. P. Yaswen and Dr. M. Stampfer, LBNL.

These latter cell lines were the epithelial breast tissue line '184' and its derivatives:

184	- a breast epithelial cell line with finite life span
184B5	- an immortalized non-tumorigenic derivative
184B5 Me	- an anchorage-independent derivative of 184 B5
184A1	- a non-tumorigenic immortal variant which shows no anchorage-independent growth
184A1TH	- a tumorigenic anchorage-independent derivative of 184A1 that arose after large SV40 T-antigen and H-ras transformation

We began to clone and characterize the tk genes expressed in seven of the eleven cell lines. Using mixed base oligonucleotides specific for conserved domains in the catalytic domains of tk genes in the PCR assays, we amplified specifically ~160-170 bp fragments of expressed tk genes. We then size selected and cloned teh PCR products into a suitable plasmid vector (pAmp1) using commercially available kit (UDG cloning kit; Gibco/Life Technologies). Ampicillin resistant clones were picked from agar plates and their insert sizes were determined by agarose gel analysis of PCR products generated with vector-specific PCR primers. DNA was isolated from the clones, bound to filters and prescreened with probes prepared from known tk genes. As of August 28, 2000, we had 172 tk fragment clones derived from breast cancer cell lines and about 250 tk fragment clones from studies of radiation-induced thyroid cancers in the prescreening and sequencing steps. Following the pre-screening with known tk fragments, we performed cDNA sequencing and database searches and added novel clones to the panel of expressed tk gene fragments. DNA isolated from this panel of tk gene fragments is then arrayed and printed onto glass slides or nylon filters to measure tk gene expression in cell lines, normal and tumor tissues.

During the report period, we finished the construction and test of a robotic system capable of printing DNA microarrays with about 100 different sequences on glass slides. The arrayer (Fig.1) can print on up to 91 slides in a single run. Typically, we print approximately 50 slides per run, with duplicate arrays on each slide. The stainless steel printing pin has an open slit in the tip cut by 0.001 inch Electrical Discharge Machining (EDM) wire - a tool commonly employed in precision semiconductor manufacturing. Each loading takes up approximately 1 μl and allows

continuous printing of more than 100 dots due to the capillary function. A full 384-well plate of DNA samples can be arrayed onto 50 slides (in duplicate) in 8 hrs, including the time needed for repeated wash and drying steps in each printing cycle. This arrayer can print more complex DNA arrays in the same time frame if more printing pins are installed. For example, 12,288 clones can be printed in the same time interval with 32 pins loaded in the print head. When the DNA is dissolved at a concentration of 250ng/μl in 50% dimethyl sulfoxide (DMSO) printing solution, spot diameters on poly-l-lysine coated slides range from 80-125 μm. The arrayer has an precision of approximately 15μm, therefore, an array with 200μm center-to-center is sufficiently spaced.

The fabrication of tyrosine kinase (tk) cDNA arrays on glass slides was done in house using the above mentioned DNA micro-arrayer. Standard microscope glass slides were thoroughly cleaned with concentrated sodium hydroxide and ethanol before coating with poly-l-lysine. These two chemical steps provided a positively charged layer to bind DNA to the slides. The coated slides were stored in closed slide boxes two weeks before they were used for printing. This "aging" process proved to promote surface chemistry of the slides for better array spot morphology. We also evaluated surface treated slides for DAN micro-array printing from different vendors, but concluded that in house prepared poly-L-lysine coated slides showed superior DNA binding and lowest levels of autofluorescence.

The printed slides were subjected to post printing processing. The locations of arrays were marked on the reverse side of the slide with diamond marker pen since the array will become invisible after processing. The slides were placed up side down in re-hydration chamber filled with 1X SSC. 5-15 minutes (depending on the size of the array) were allowed for array to re-hydrated until spots were glistening but care should be taken not to allow spots to swell too much and run into each other. Hydrated slides were placed on a heat plate pre-set to 70 ^{0}C for 3 seconds to snap-dry the array. These slides were then cross-linked by an UV cross linker (such as Stratalinker 1800 or 2400, Stratagene Inc.) at 65 mJ. Cross-linking was optional, however, it did promote the bonding of DNA onto the poly-l-lysine coating. After cross-linking, slides were incubated in a blocking solution consisting of 0.21M succinate anhydride in 1-methyl-2-pyrrolidinone, 0.06M sodium borate for 20 minutes (pH=8). A boiling water bath was prepared during this time, and the slides were denatured in the boiling water for 2 minutes after blocking by quickly plunging up and down. The denatured arrays were then submerged in a 95% ethanol bath with plunging up and down for 1 minute. This step de-hydrated the denatured DNA and allowed them to remain single-stranded. An immediate centrifuge at 500 rpm for 5 minutes was performed to remove any trace ethanol or water. The arrays were then ready for hybridization.

Quality control for the tk arrays was monitored throughout the tk array fabrication process. Since dust can be a major source of background fluorescence, a dust-reduced printing and processing

environment minimized these interfering particles and reduced background. All reagents used for printing and coating of slides were prepared fresh and filtered. Before post-printing processing of the arrays, morphology of the spot and DNA distribution within the spots were examined with DAPI staining and visualized in a Zeiss fluorescence microscope. After post-printing processing, arrays were stained with POPO-3 dye (0.01 mM) and scanned at Cy3 channel to ensure the retention of DNA on the arrays for hybridization.

A Zeiss Axioplan II Mot fluorescence microscope was programmed to acquire an fluorescence image of arrays of 10x10 spots in 9 image frames. Image stitching and processing were automated by macros to show details of spots with 1 micron resolution. While being less sensitive than commercial DNA microarray scanners, the system is being used routinely for quality control of each batch of new arrays.

To facilitate printing of DNA on nylon filters for recombinant clone screening, we designed a printing tool that can be mounted on the Beckman Biomek 1000 robot in our laboratory. The tool (Fig.2) can hold up to 32 steel pins arranged so that they fit directly into the wells of a 384-well microtiter plate. The slotted pins (purchased from V&P Scientific, San Diego, CA) carry about 50 nl of liquid. The entire volume is deposited in one spot on a positively charged nylon filter. The pins needs to be refilled prior to each print step. In between DNA samples, the print pins are washed thoroughly and blot dried. The system is capable to array a 96 well microtiter plate in a little more than 1 hour spotting all 96 wells in duplicate and printing three such micro-arrays. We presently compare the sensitivity of hybridization to the filter bound arrays with the results obtained with glass bound arrays.

It was necessary to adjust hybridization and wash conditions to obtain specificity and reduce background fluorescence to a level where quantitative information could be obtained. The slides were placed inside hybridization chambers with cover glass fastened tightly by clamps. Multiple drops of 3xSSC were added around the arrays on the slide to maintain the humidity and prevent drying of hybridization solution. Hybridization was performed under glass coverslips overnight at 65 ^{0}C. The arrays were then washed in 3 changes of wash solution (1xSSC+ 0.03% SDS) at room temperature for 5 minutes, 0.2xSSC at room temperature for 1 minute, and then 0.2xSSC at 50 ^{0}C for 1 minute. After the washes, the slides were dried immediately by centrifugation at 500 rpm for 5 min before scanning. Currently, sample preparation and hybridization procedures have produced signal to background (noise) ratios of approximately 30 (in green channel) to 40 (in red channel). This dynamic range can be further improved by the reduction of background fluorescence.

We also began to develop algorithms for array readout and comparisons between measurements. An Axon GenePix 4000 (Axon Inc.) array scanner was used to acquire all images. This scanner has a preview resolution of 40 μm and a scanning resolution of 10 μm. PMT power can be adjusted by

the user during previewing to optimize the signal intensity. GenePix 3.0 (Axon Inc.), an image acquisition software, was used to analyze the acquired images and to provide numerical data that can be imported into spreadsheets for further analysis. For display purposes, the images can be saved in standard formats and imported into common graphics programs such as Adobe Photoshop.

The performance of the system was tested by hybridization of fluorochrome-labeled tk gene-specific PCR fragments onto the tk-specific DNA micro-arrays. These preliminary experiments allowed us to optimize hybridization and wash conditions, and to generate data regarding the relative level of gene expression. For example, when hybridizing a combination of Cy3-labelled tk fragments prepared from cell line 181A1 and Cy5-labelled tk fragments prepared from cell line 181A1TH to a DNA micro-array carrying 58 tk gene fragments, scanning the array and displaying Cy3 fluorescence signals in green and Cy5 signals in red, difference between the cell lines became apparent (Fig.3). Genes expressed at higher a level in 181A1TH cells lead to increased green signals on the array, while those genes whose expression level is lower in 181A1TH cells compared to 181A1 cells generated spots that exhibited stronger red fluorescence (Fig.3). The image in Fig.3 shows the hybridization results using 2 almost identical micro-arrays. Each 67 spot array carries 58 tk gene fragments, six Cy3- or Cy5-labelled control DNAs and three spot carrying housekeeping genes. The upper array in Fig.3 lacks a few spots, most likely due to surface inhomogeneities. This problem did not recur in more recent printing runs. The position of four clones in the second row of the arrays was switched. This, however did not affect the analysis.

The Genepix software provided quantitative information about CY3 and CY5 fluorescence intensities for each of the spots, which allowed us to calculate fluorescence intensity ratios. Table 1 (Appendix 1) lists the fluorescence intensity values for each spot (except the controls). The spots are identified by the tk fragment clone number, each of which is specific for a particular tyrosine kinase. Table 1 also lists the values after background subtraction and normalization (Cy5 norm., Cy3 norm.), the CY3/Cy5 ratio of each spot that showed sufficient hybridization intensity as well as an average ratio printed in bold. In our preliminary analysis, we defined gene as being up-regulate or down-regulated in the tumorigenic cell line when the average Cy3/Cy5 ratio exceeded 2.0 or fell under 0.4, respectively. Using these arbitrary cut-off values, we found eight genes with altered expression in 181A1TH. The expression of three gene appeared down-regulated, while five genes appeared up-regulated in the large T antigene/H-ras transformed cells. The eight genes represent various receptor tyrosine kinase genes, among them members of the family of ephrin receptor. This makes sense, since some ephrin receptors have been shown to be involved in cell adhesion and cell-cell interaction. We will performed RNA in situ hybridization experiments with differently labeled cDNA probes to confirm these results prior to publication.

KEY RESEARCH ACCOMPLISHMENTS:

- Finished the construction and test of a robotic system to prepare DNA micro-arrays on glass slides
- Finished the design, assembly, programming and test of a robotic system to prepare DNA micro-arrays on nylon filters
- Finished the design and programming of a microscope-based digital imaging system to acquire high resolution images for quality control of fluorescently stained DNA micro-arrays
- Molecularly cloned cDNA preparations enriched in tyrosine kinase gene fragments in plasmid vectors, commenced insert sequencing and expanded the panel of tyrosine kinase genes used for expression profiling
- Demonstrated the feasibility of tk gene expression profiling after RT-PCR using breast cancer cell lines
- Demonstrated tk gene expression changes as breast epithelial cells become tumorigenic and grow anchorage-independant

REPORTABLE OUTCOMES:

- **manuscripts**

1. K.M. Greulich, L. Kreja, B. Heinze, A. P. Rhein, H.-U.G. Weier, M. Brückner, P. Fuchs, M. Molls Rapid detection of radiation-induced chromosomal aberrations in lymphocytes and hematopoietic progenitor cells by M-FISH. Mutation Res 452:73-81
2. Weier, H.-U.G., Munné, S., Lersch, R.A., Hsieh, H.B., Smida, J., Chen, X.N, Korenberg, J.R., Pedersen, R.A., Fung J. (2000) Towards a Full Karyotype Screening of Interphase Cells: 'FISH and Chip' Technology. Molecular and Cellular Endocrinology (submitted)

- **presentations**

1. Hsieh, H.B., Weier, H.-U.G. "DNA Microarray for Gene Expression Profiling of Human Tumors", Seminar in Academia Sinica, Taiwan, Jan 6, 2000.
2. Hsieh, H.B., Weier, H.-U.G. "Expression Profiling of Tyrosine Kinase Genes by FISH and Chips", The Histochemical Society 51th Annual Meeting, New Orleans, LA, March 24-26, 2000.
3. Hsieh, H.B., Weier, H.-U.G. "Kinase Gene Expression Profiling-Instrumentation & Prototype Setup", Oral presentation in Corning Inc., Corning, NY, May 8, 2000.
4. Hsieh, H.B., Weier, H.-U.G. "Kinase Gene Expression Profiling in Human Tumors", Subcellular Structure Department Seminar, Life Science Division, E.O. Lawrence Berkeley National Laboratory, May 10, 2000.
5. Weier, H.-U.G. (2000) Towards a Full Karyotype Screening: SKY, chip technology. Third International Symposium on Pre-Implantation Genetic Analysis. Palazzo di Congressi, Bologna, Italy, June 22-23, 2000.

- **funding obtained**

U.S. Department of Defense Prostate Cancer Research Program, 'Tyrosine Kinase Gene Expression Profiling in Prostate Cancer', New Investigator Award, H.-U. Weier (P.I.), 4/01/00-3/31/03

CONCLUSIONS:

This 3-year IDEA project is well on track and, although most of its initial milestones were to be met after 18 months, the preliminary results have already proven the hypothesis that changes in tk gene expression can be monitored by a combination of PCR using tk gene family-specific primers and DNA micro-arrays. The soft- and hardware components necessary for these studies were put in place in the first year. Concordant with the timeline presented in the original proposal, research and development in the second year will focus on finishing the definition of the panel of genes to be profiled, thorough studies of assays reproducibility and sensitivity, and application of the technology to clinical specimens. While the hybridization to the DNA micro-array appears to possess the required specificity, second year research will also address the issues of hybridization background reduction and definition of a suitable reference DNA probe.

REFERENCES:

None

APPENDICES:

1. Figures 1 and 2
2. Figure 3 and Table 1
3. Table 1 (continued)
4. K.M. Greulich, L. Kreja, B. Heinze, A. P. Rhein, H.-U.G. Weier, M. Brückner, P. Fuchs, M. Molls Rapid detection of radiation-induced chromosomal aberrations in lymphocytes and hematopoietic progenitor cells by M-FISH. Mutation Res 452:73-81
5. Weier, H.-U.G., Munné, S., Lersch, R.A., Hsieh, H.B., Smida, J., Chen, X.C., Korenberg, J.R., Pedersen, R.A., Fung J. (2000) Towards a Full Karyotype Screening of Interphase Cells: 'FISH and Chip' Technology. Molecular and Cellular Endocrinology (submitted)

Figure 1: This DNA micro-arrayer built in our laboratory allows to print duplicate arrays on up to 91 slides. When in operation, the instrument is enclosed to maintain a mostly dustfree enviroment with controlled humidity.

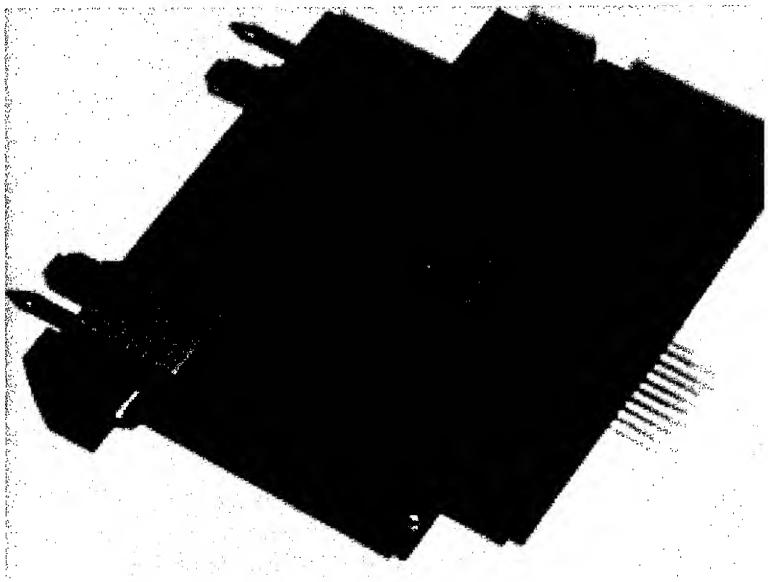

Figure 2: This DNA micro-arrayer tool fits onto our Beckman Biomek 1000 laboratory robot. Its 32 pin capacity allows rapid printing on glass or nylon membranes directly out of 384 well microtiter plates. Each pins carries about 50 nanoliters of liquid.

Appendix 2

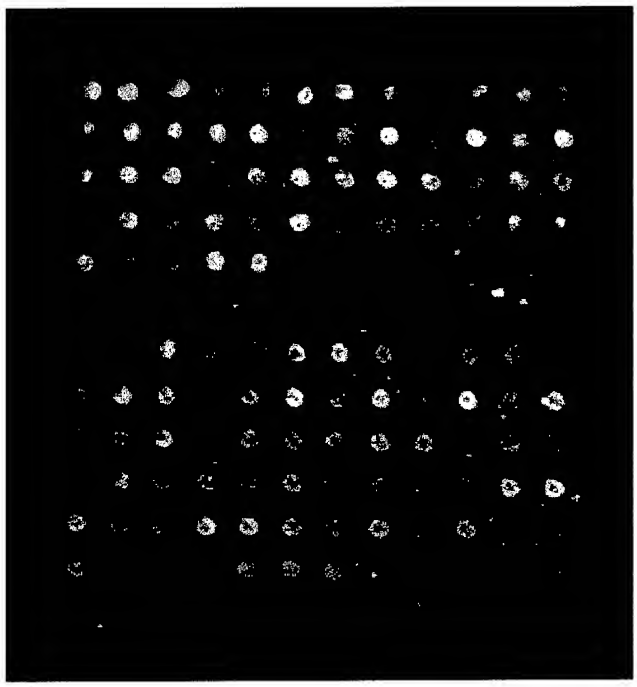

Figure 3: Hybridization of PCR-amplified tyrosine kinase DNA fragments onto a duplicate 67 spot DNA micro-array.

Table I: Tyrosine kinase gene expression levels in breast cancer cells lines

		ARRAY1	Cy5	Cy3	Cy3/Cy5		ARRAY2	Cy5	Cy3	Cy3/C	Av.	Comment
Target	Cy5	Cy3	norm.	norm.	ratio	Cy5	Cy3	norm.	norm.	ratio	ratio	
Ron-Cy3	control											
HPRT-Cy3	control											expression
MCF7-CY3	control											level
316/77	11361	3346	3120	1386	0.44	11711	3126	3163	1010	0.32	**0.38**	down
316/151	6306	3816	1627	1899	1.17	4363	3195	978	1274	1.30	**1.23**	
316/120	10402	5487	2852	3583	1.26	9281	4626	2430	2609	1.07	**1.16**	
289/33	9647	6614	2628	4672	1.78	7550	5829	1911	3611	1.89	**1.83**	
289/34	9131	4080	2478	2006	0.81	9117	3704	2357	1419	0.60	**0.71**	
289/233	2357	3148	474	1071	2.26	2571	2961	399	641	1.61	**1.93**	
289/78	5804	4211	1483	1789	1.21	7431	3770	1837	1598	0.87	**1.04**	
289/38	3276	5089	740	2786	3.76	2893	3845	455	1801	3.96	**3.86**	up
289/85	7333	3350	1964	920	0.47	7848	3000	1920	791	0.41	**0.44**	down
289/50	13618	3923	3834	1787	0.47	9565	3628	2572	1445	0.56	**0.51**	
289/293	8262	8168	2229	5889	2.64	5942	5748	1475	3501	2.37	**2.51**	up
289/46	9886	5314	2706	3120	1.15	7579	4508	1936	2294	1.18	**1.17**	
316/181	14547	4568	4047	2390	0.59	7584	3416	1924	1235	0.64	**0.62**	
182/106	12030	6049	3299	3882	1.18	7879	3843	1981	1682	0.85	**0.42**	
289/119*	14126	5088	3904	2935	0.75	10798	5836	2829	3719	1.31	**1.15**	
289/22	3666	2981	800	785	0.98	6442	3619	1482	1427	0.96	**1.00**	
316/70	7947	4248	2081	2142	1.03	9154	5140	2268	2866	1.26	**1.22**	
289/152	3696	3505	829	1265	1.53	3524	3478	557	989	1.78	**1.65**	

* Cross-contamination between clones 289/119 and 289/61 in Array 2.

Appendix 3

Table 1 ontinued

Target	Cy5	ARRAY1 Cy3	Cy5 norm.	Cy3 norm.	Cy3/Cy5 ratio	Cy5	ARRAY2 Cy3	Cy5 norm.	Cy3 norm.	Cy3/Cy ratio	Av. ratio	Expression level
316/178	11609	6516	3190	4090	1.28	11663	6283	2978	3749	1.26	**1.27**	
316/160	8946	4822	2356	2283	0.97	6113	3753	1252	1315	1.05	**1.01**	
289/357	10674	6284	2894	3730	1.29	7910	4875	1738	2292	1.32	**1.30**	
316/137	15537	4082	4378	2141	0.49	7230	3386	1828	1221	0.67	**0.58**	
182/138	12367	5827	3431	3683	1.07	5626	3814	1309	1602	1.22	**1.15**	
182/151	7193	6615	1892	4300	2.27	4629	4286	976	1993	2.04	**2.16**	up
289/382	2844	3300	568	1031	1.82	2720	3076	377	739	1.96	**1.89**	
289/267	10079	3912	2668	1629	0.61	8958	3746	2208	1318	0.60	**0.60**	
289/44	10134	5151	2684	2945	1.10	6224	3771	1352	1387	1.03	**1.06**	
182/79	6315	4486	1504	2189	1.46	5407	3880	1064	1558	1.46	**1.46**	
316/18	9994	5800	2590	3429	1.32	7069	4283	1509	1965	1.30	**1.31**	
316/61	6853	4776	1651	2364	1.43	5032	4122	870	1574	1.81	**1.62**	
289/131	8146	3626	2059	1149	0.56	6939	2816	1423	284	0.20	**0.38**	down
289/84	5423	4538	1248	1979	1.59	4338	3675	579	1122	1.94	**1.76**	
289/113	6108	4117	1447	1599	1.10	4612	3456	602	691	1.15	**1.13**	
289/257	2025	2666	340	701	2.06	2316	3116	413	1015	2.46	**2.26**	up
289/53	7047	4947	1823	2863	1.57	5394	4371	1231	2146	1.74	**1.66**	
289/247	2970	3722	603	1461	2.42	3129	3701	507	1395	2.75	**2.59**	up
289/353	5537	4437	1350	1907	1.41	4774	3612	974	1173	1.20	**1.31**	
182/41	3797	3600	803	1108	1.38	4033	3398	715	893	1.25	**1.31**	
289/61*	9996	7179	2632	4788	1.82	4605	3869	861	1336	1.55*	**1.68**	
289/184	4849	3073	1038	696	0.67	5491	3120	1061	724	0.68	**0.68**	
289/18	3593	3713	651	1272	1.95	4295	3448	631	1012	1.60	**1.78**	
316/232	5385	3504	1175	1042	0.89	5634	3548	969	836	0.86	**0.87**	
289/476	6165	3523	1393	1274	0.91	5553	3572	902	882	0.98	**0.95**	
289/39	6961	4374	1624	2210	1.36	7062	4645	1298	1840	1.42	**1.39**	
289/49	5396	3069	1160	905	0.78	11219	4841	2401	1941	0.81	**0.79**	
316/39	8895	4593	2388	2679	1.12	8518	4485	2224	2481	1.12	**1.12**	
316/103	4359	4095	1028	2071	2.01	3852	3625	761	1337	1.76	**1.89**	
316/91	5478	3720	1353	1552	1.15	4574	3560	916	1176	1.28	**1.22**	
404/007	11173	5909	3032	3564	1.18	8398	4684	2026	2209	1.09	**1.13**	
404/008	9996	5161	2664	2910	1.09	7352	4307	1664	1696	1.02	**1.06**	
404/027	1188	2557	9	278		6694	3929	1452	1309	0.90	**0.45**	
404/032	1321	2251	6	-208		3727	3437	503	840	1.67	**0.84**	
404/053	1331	2600	-1	109		6080	4244	1179	1627	1.38	**0.69**	
404/174	1511	2302	36	-47		3605	3253	384	577	1.50	**0.75**	
289-157	5108	3306	1019	1105	1.08	6374	4053	1141	1345	1.18	**1.13**	
289-176	1528	1943	-19	-68		3319	2459	170	-258		**0.00**	
289-187	1528	2050	4	-5		3250	2964	49	180	3.67	**1.84**	
404-19	833	1850	-3	0		6044	3967	1453	1742	1.20	**0.60**	
430/1	964	2078	8	-5		1408	2584	-2	269		**0.00**	
433/2	1032	2280	15	33		1696	2814	46	457		**0.00**	
436/2	1031	2135	-2	-19		1512	2678	-14	224		**0.00**	
arg-CY3	control											
BH281CY3	control											
Bh258CY3	control											

* Cross-contamination between clones 289/119 and 289/61 in Array 2.

Appendix 4

ELSEVIER

Mutation Research 452 (2000) 73–81

Fundamental and Molecular Mechanisms of Mutagenesis

www.elsevier.com/locate/molmut
Community address: www.elsevier.com/locate/mutres

Rapid detection of radiation-induced chromosomal aberrations in lymphocytes and hematopoietic progenitor cells by mFISH

K.M. Greulich [a,*], L. Kreja [b], B. Heinze [c], A.P. Rhein [a], H.-U.G. Weier [d], M. Brückner [a], P. Fuchs [e], M. Molls [a]

[a] *Department of Radiation Oncology, Technical University of Munich, Ismaninger Strasse 22, D-81675 Munich, Germany*
[b] *Institute for Occupational, Social and Environmental Medicine, University of Ulm, Ulm, Germany*
[c] *Department of Medical Genetics, University of Ulm, Ulm, Germany*
[d] *Life Sciences Division, E.O. Lawrence Berkeley National Laboratory, Berkeley, CA, USA*
[e] *Vysis GmbH, Bergisch-Gladbach, Germany*

Received 7 July 1999; received in revised form 11 February 2000; accepted 3 April 2000

Abstract

Structural chromosome aberrations (SCAs) are sensitive indicators of a preceding exposure of the hematopoietic system to ionizing radiation. Cytogenetic investigations have therefore become routine tools for an assessment of absorbed radiation doses and their biological effects after occupational exposure or radiation accidents.

Due to its speed and ease of use, fluorescence in situ hybridization (FISH) with whole chromosome painting (WCP) probes has become a method of choice to visualize SCAs. Until recently, this technique was limited to a rather small number of chromosomes, which could be tested simultaneously. As a result, only a fraction of the structural aberrations present in a sample could be detected and the overall dose effect had to be calculated by extrapolation. The recent introduction of two genome-wide screening techniques in tumor research, i.e., Spectral Karyotyping (SKY) and multicolor FISH (mFISH) now allows the detection of translocations involving any two non-homologous chromosomes.

The present study was prompted by our desire to bring the power of mFISH to bear for the rapid identification of radiation-induced SCAs. We chose two model systems to investigate the utility of mFISH: lymphocytes that were exposed in vitro to 3 Gy photons and single hematopoietic progenitor cell colonies isolated from a Chernobyl victim 9 years after in vivo exposure to 5.4 Sv.

In lymphocytes, we found up to 15 different chromosomes involved in rearrangements indicating complex radiation effects. Stable aberrations detected in hematopoietic cell colonies, on the other hand, showed involvement of up to three different chromosomes. These results demonstrated that mFISH is a rapid and powerful approach to detect and characterize radiation-induced SCAs in the hemopoietic system. The application of mFISH is expected to result in a more detailed and, thus, more informative picture of radiation effects. Eventually, this technique will allow researchers to rapidly delineate

* Corresponding author. Tel.: +49-89-4140-4415; fax: +49-731-960-8554.
E-mail address: kgreulich@primus-online.de (K.M. Greulich).

0027-5107/00/$ - see front matter
PII: S0027-5107(00)00057-9

chromosomal breakpoints and facilitate the identification of the genes involved in radiation tumorigenesis. © 2000 Published by Elsevier Science B.V.

Keywords: Radiation; Chromosome aberrations; Hematopoietic system; Stem cells; mFISH; Chernobyl accident

1. Introduction

Fluorescence in situ hybridization (FISH) using several differently labeled whole chromosome painting (WCP) probes has become the method of choice for the detection of radiation-induced chromosomal aberrations [1–5]. Unstable aberrations such as dicentric chromosomes can easily be distinguished from the stable and thus heritable rearrangements by inclusion of centromeric marker probes in the hybridization reaction [6,7]. The steadily increasing application of the chromosome painting technique for the detection of structural chromosome aberrations (SCAs) in cells following irradiation or exposure to chemical clastogens has also lead to a new nomenclature to describe the observed chromosomal changes [8,9].

There are, however, limitations for the detection of SCAs by chromosome painting. Conventional fluorescence microscopes used to score aberrations are equipped with filter sets that allow to discriminate no more than three or four different fluorescent reporter molecules [10,11]. Consequently, the assays to detect SCAs are based on staining a subset of the human chromosome set and calculating the total number of aberrations per cell by linear extrapolation [3,4,12].

Recent improvements in detection technology now allow an extended number of chromosomes to be analyzed simultaneously in the same metaphase spread. Two techniques available for the analysis of spreads hybridized with 24 different human-specific WCP probes are the interferometer based 'Spectral Karyotyping' (SKY) system [13] and the filter based 'multicolor FISH' (mFISH) approach [14]. The SKY technology has been applied very successfully to the analysis of cytogenetic changes in tumor cells [15,16] and, more recently, to the analysis of interphase cells [17]. However, the SKY system generates a rather large amount of data by measuring complete fluorescence spectra for each point in the image [13]. This severely limits the system's throughput, and may compromise productivity when analyzing cells populations with mostly normal and few aberrant cells. We studied the filter-based mFISH technique to develop assays that will eventually measure radiation damage with high accuracy and allow to predict radiation tolerance.

Metaphase spreads prepared from short term cultures of peripheral blood lymphocytes (PBLs) have previously been used in biological dosimetry to study radiation effects in vitro [18]. Furthermore, FISH on PBLs has been used to evaluate assays to determine the individual radiosensitivity of radiotherapy patients [19]. Lymphocytes, however, are not the only target for radiation damage within the hematopoietic system. Hematopoietic stem cells isolated by a colony assay have been suggested to be more appropriate for elucidating the immediate as well as the late effects of radiation exposure [20,21]. However, preparations of dividing single hematopoietic progenitor cells [22–24] lack the quality and quantity of metaphase spreads to successfully apply conventional cytogenetic techniques, i.e., banding analysis [25].

We have shown previously that two- or three-color FISH can be successfully applied to metaphase spreads of single hematopoietic colonies. But since the chromosomal damage is a statistical event and thus unpredictable in single colonies, a complete identification of chromosomes involved in marker chromosome formation could not be achieved [25].

The present study was initiated to analyze aberrant chromosomes in PBLs after in vitro exposure to 3 Gy photons and in single hematopoietic colonies derived from a Chernobyl nuclear accident victim 9 years after exposure to 5.4 Sv.

2. Material and methods

2.1. Lymphocyte cultures

Heparinized peripheral blood samples from five healthy individuals (3 males, 2 females, age range: 32–35 years) were exposed to single doses of 3 Gy

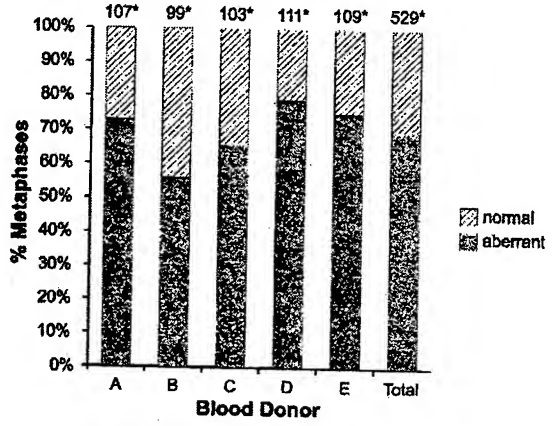

Fig. 1. mFISH analysis of metaphases derived from lymphocytes after in vitro exposure to 3 Gy photon irradiation. *Absolute number of analyzed metaphases per donor.

irradiation (photons, low LET, 6 MeV, 2.8 Gy/min, Siemens MX-2, Germany). Short-term cultures set up from the irradiated blood samples as well as from non-irradiated controls were cultured for 72 h. Metaphase spreads were prepared following a standard protocol [26].

2.2. Hemopoietic progenitor cells

Investigations on radiation-induced, long-term persisting SCAs in hematopoietic cells were performed on blood samples from a Chernobyl accident victim (male, born in 1950, patient #1011 in the Moscow-Ulm Radiation Accident History Data Base (MURAD, [27]). This individual was reportedly exposed to 5.4 Sv during the 1986 accident. Nine years after the accident, peripheral blood samples were cultured to obtain hematopoietic stem cell colonies. Methylcellulose cultures stimulated with recombinant hematopoietic growth factors (interleukin 3, stem cell factor and erythropoietin) were set up with cryopreserved low density mononuclear PBLs separated by a Ficoll gradient (density 1.077 g/ml). Cell culture and preparation of metaphase spreads from single colonies were performed as described [25].

2.3. mFISH experiments

We applied mFISH [14] to metaphase spreads prepared from short term lymphocyte cultures and from hematopoietic colonies using the Spectra Vysion™ system (Vysis, Bergisch-Gladbach, Germany). mFISH using commercially available WCP probes was performed following the manufacturer's (Vysis) instructions. Hybridized metaphase spreads were analyzed using a computer-assisted fluorescence microscope (Axioplan 2, Zeiss, Göttingen, Germany). The images were recorded with a CCD camera (Photometrics, Tucson, AZ, USA) and pictures were analyzed with the Quips SpectraVysion™ Software (Vy-

Table 1
Results of mFISH analysis of metaphases derived from lymphocytes after in vitro exposure to 3 Gy photon irradiation

Number of aberrant chromosomes per metaphase	Fraction of metaphases carrying aberrant chromosomes					
	Donor A	Donor B	Donor C	Donor D	Donor E	Total
One Chr	7/78	3/55	4/68	12/88	8/82	34/371
Two Chr	28/78	21/55	28/68	29/88	32/82	138/371
Three Chr	9/78	12/55	13/68	17/88	11/82	62/371
Four Chr	8/78	9/55	7/68	12/88	12/82	53/371
Five Chr	8/78	7/55	3/68	6/88	10/82	34/371
Six Chr	4/78	2/55	9/68	3/88	4/82	22/371
Seven Chr	3/78	1/55	2/68	3/88	2/82	11/371
Eight Chr	3/78	0/55	2/68	1/88	1/82	7/371
Nine Chr	2/78	0/55	0/68	3/88	0/82	5/371
Ten Chr	0/78	0/55	0/68	2/88	1/82	3/371
Eleven Chr	1/78	0/55	0/68	0/88	0/82	1/371
Twelve Chr	0/78	0/55	0/68	0/88	0/82	0/371
Thirteen Chr	0/78	0/55	0/68	0/88	0/82	0/371
Fourteen Chr	0/78	0/55	0/68	0/88	0/82	0/371
Fifteen Chr	0/78	0/55	0/68	0/88	1/82	1/371

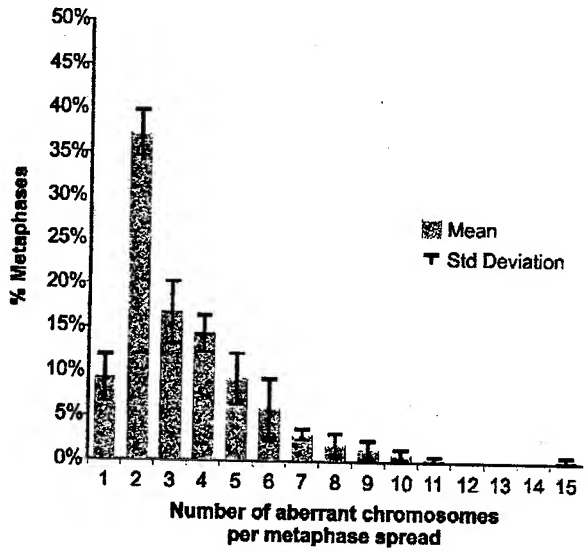

Fig. 2. Number of chromosomes involved in aberrations within a single metaphase of in vitro irradiated lymphocytes (3 Gy). The mean (in % of metaphases) +/− standard deviation observed in five healthy individuals is presented (100% = 371 aberrant metaphases).

sis, now distributed through Applied Imaging). On average, we analyzed 100 metaphases from the in vitro irradiated lymphocytes, and 20 metaphases from each non-irradiated control. From the hematopoietic progenitor cells, two BFU-E colonies (burst forming unit-erythroid) were analyzed by scoring 20 and 26 metaphases per colony.

3. Results

3.1. In vitro irradiated lymphocytes

Our mFISH analysis of the non-irradiated blood samples from five apparently healthy individuals revealed neither structural nor numerical chromosome aberrations (data not shown).

After in vitro exposure to 3 Gy photons, abnormalities were found in 56–79% of metaphases prepared from lymphocyte cultures (mean value: 70% for all five donors) (Fig. 1). Detailed analysis of 371

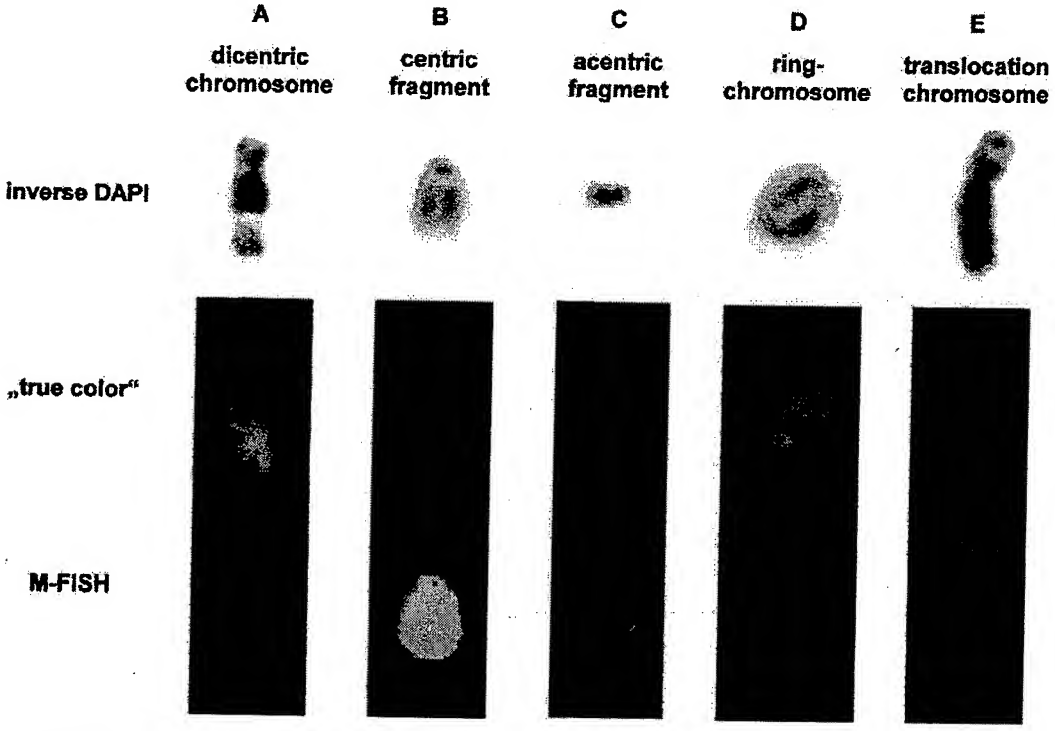

Fig. 3. Results of mFISH applied to in vitro irradiated (3 Gy) lymphocytes. For representative radiation-induced chromosomal aberrations, the inverted DAPI-banding pattern, the RGB composite hybridization image and the resulting pseudo-colored mFISH image are shown. (A) A dicentric chromosome composed of chromosome 4 (pseudo-color: dark blue) and chromosome 9 (pseudo-color: light blue) material, (B) A centric fragment of chromosome 7 (pseudo-color: yellow), (C) An acentric fragment of chromosome X (pseudo-color: pink), (D) A ring chromosome 5 (pseudo-color: purple), and (E) One of the products of a reciprocal translocations involving chromosome 4 (pseudo-color: dark blue) and chromosome 18 (pseudo-color: brown).

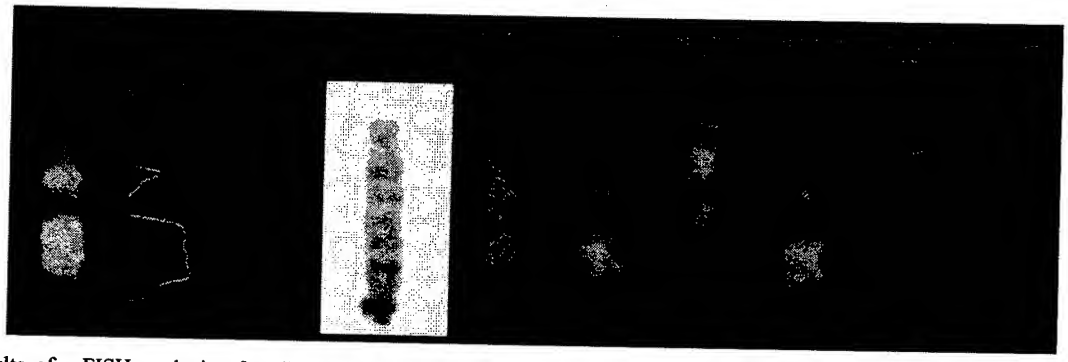

Fig. 4. Results of mFISH analysis of a dicentric chromosome consisting of an alternating combination of chromosome 17–15–17–15 material: displayed are the inverted DAPI-banding pattern, the RGB color composite hybridization image and the resulting pseudo-colored mFISH image. The hybridization signals for each individual color are shown in single fluorescent color projections. Each chromosome-specific DNA is characterized by a unique combination of fluorescent colors. For example chromosome 17 material has bound red, green and FRed labeled probes.

aberrant metaphases revealed that in 138 cells (37.2%) two chromosomes were involved in aberrations. In 194 of 371 spreads (52.3%), between 3 and 9 chromosomes participated in rearrangements. As many as 5 of 371 metaphases (1.3%) (Table 1, Fig. 2) contained multiple aberrations involving 10–15 chromosomes. Typical SCAs found in metaphase spreads are shown in Fig. 3A–E. We observed unstable chromosomal aberrations such as dicentric chromosomes (Fig. 3A), centric and acentric fragments (Fig. 3B and C), ring chromosomes (Fig. 3D) as well as stable chromosomal aberrations (Fig. 3E). In each

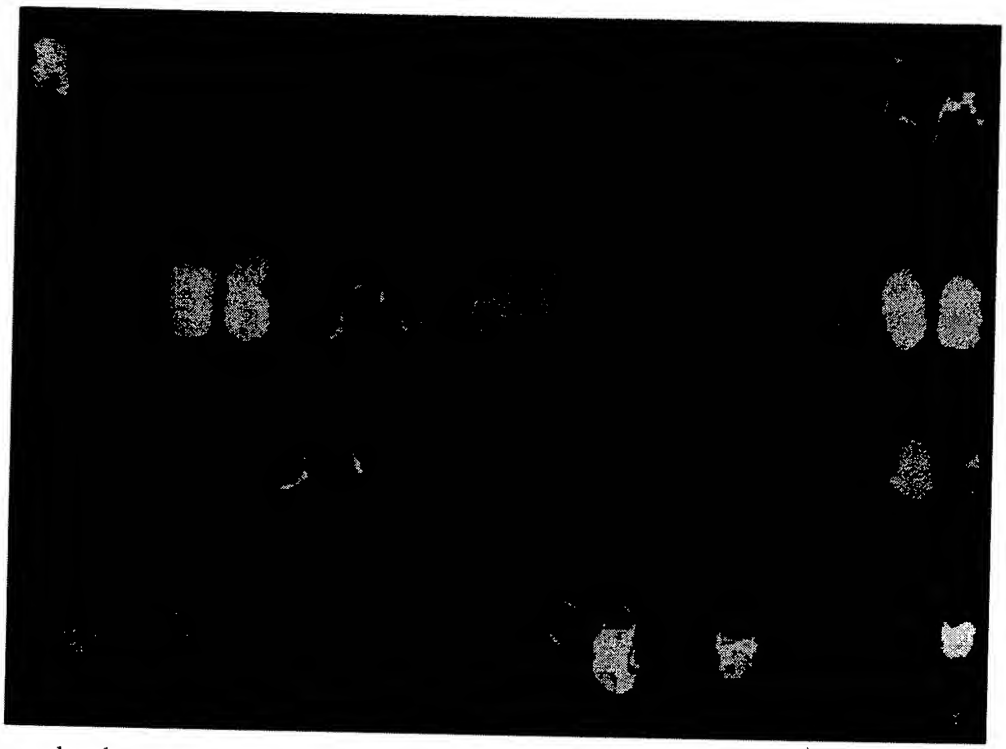

Fig. 5. A cell from a lymphocyte culture analyzed by mFISH showing 15 different chromosomes involved in complex radiation induced aberrations (chromosomes 1,3, 4, 5, 8, 10, 11, 14, 16, 18, 19, 20, 21, 22 as well as X). This cell carried centric fragments of chromosome 1, 3, and 4, a centric and an acentric fragment of chromosome 8, a dicentric chromosome (4;5) and the following translocations: t(21;1), t(11;19), t(16;3), t(19;14), t(20;18), t(22;1), t(X;18;X), t(10;X), t(14;4).

instance, the chromosomes involved in the translocation could be identified unambiguously in a single hybridization experiment.

An example of a complex chromosomal rearrangement is presented in Fig. 4, which also illustrates the mFISH analysis procedure. An image showing the inverted DAPI banding pattern helped us to identify a marker chromosome resembling a dicentric chromosome with somewhat regular light and dark bands. The display of the five different fluorescent images revealed the chromosomal make-up of this marker, i.e., the origin of the different parts of the chromosome. Chromosome 17 material, for example, was identified by a unique combination of red, green and FRed, e.g., far red, fluorescent signals. The profile display showed a calculated average fluorescence signal intensity along the axis of the chromosome. This dicentric chromosome consisted of material derived from chromosomes 17 and 15 in an alternating sequence of 17–15–17–15 material. This is an example for a cryptic chromosomal aberration.

Fig. 5 represents a metaphase spread in which the 15 different chromosomes were found involved in a very complex radiation-induced karyotype. The chromosomes 1, 3, 4, 5, 8, 10, 11, 14, 16, 18, 19, 20, 21, 22 as well as chromosome X were found rearranged. This cell carried centric fragments of chromosome 1, 3, and 4, a centric and an acentric fragment of chromosome 8, a dicentric chromosome t(4;5) as well as the following translocations: t(21;1), t(11;19), t(16;3), t(19;14), t(20;18), t(22;1), t(X;18;X), t(10;X), and a t(14;4).

3.2. *In vivo irradiated hemopoietic stem cells*

Analysis of two hematopoietic BFU-E colonies derived from a Chernobyl victim showed that the application of mFISH is possible even on single methylcellulose isolated colonies. In both colonies, clonal markers (found in all mitoses from a single colony) were identified after chromosome group analysis of Giemsa stained slides.

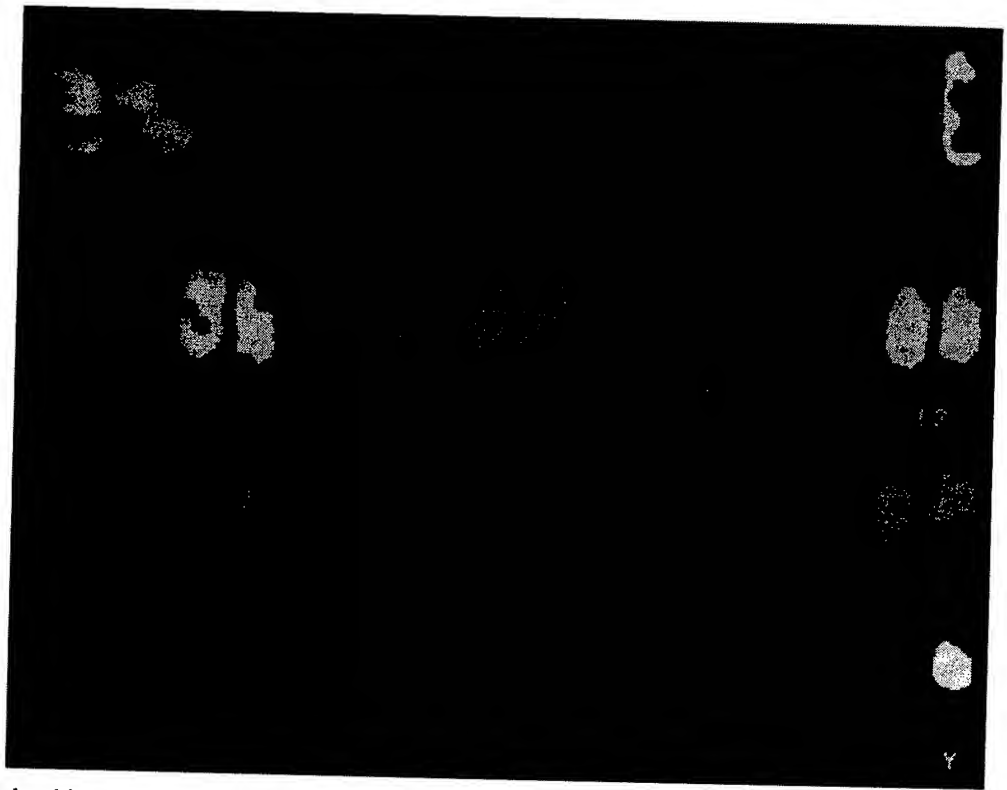

Fig. 6. Pseudo-colored image of an incomplete metaphase of a BFU-E colony (hemopoietic erythroid progenitor) derived from peripheral blood of a Chernobyl victim 9 years after radiation exposure. This karyotype can be described as 44, XY, 17q −, t(20;18;17), $-D_{13}$, $-F_{20}$.

From the first colony, 26 images were analyzed. Since the micromethod for chromosome preparation of hematopoietic stem cells produces a fair amount of incomplete metaphases with random loss of chromosomes [24,25], a complete karyotype to define the consistent aberrations was assembled by combining the results from several metaphases. Fig. 6 shows a pseudo-color image of a typical incomplete metaphase, which was identified as 44, XY, 17q −, t(20p;18q;17q), − D_{13}, − F_{20}. All other aberrant metaphases of this colony showed the same marker chromosome, carried two normal copies of chromosomes 13 and one normal chromosome 20. It could thus be concluded that this colony was carrying a t(20p;18q;17q) as well as a deleted chromosome 17q as stable, radiation-induced chromosomal aberrations. The resulting complete karyotype of this colony is 46, XY, del(17)(q), t(20p;18q;17q).

In the second colony, we identified a marker chromosome which consisted of chromosome 4 and 3 material (data not shown). The resulting complete karyotype of this second colony was 46, XY, t(4,3).

In summary, we were able to confirm by mFISH the existence of a clonal marker as suggested by the chromosome group analysis (Giemsa staining). The mFISH technique allowed us to characterize these markers and identify the chromosomes involved in their formation.

4. Discussion

We have shown that mFISH is suitable to rapidly and unambiguously identify radiation-induced chromosomal abnormalities of in vitro irradiated lymphocytes and to analyze long term persisting SCAs at the hematopoietic stem cell and progenitor cell levels.

The major advantage of mFISH is the speed of the technique, which, in our hands, was about 10 times faster than classical cytogenetic analysis using chromosome banding. The reasons for this were several-fold. Probes are commercially available, the hybridization proceeds overnight, and slide washes and image acquisition are completed within 2 h. Furthermore, cytogenetic expertise is very helpful but not necessary for the analysis of mFISH experiments.

The disadvantages are that the technique needs to be optimized for the target material in order to obtain optimal hybridization quality, and that the results need to be double-checked. An example of the performance of the mFISH analysis is shown in Fig. 4 for a dicentric chromosome. The inverted DAPI-banding pattern allows the identification of centromeres or satellites and helps to check the suggested mFISH results by the means of classical cytogenetics. This is important for the analysis when only metaphases with 46 centromeres are to be scored or the visualization of the centromeres is necessary to discriminate between symmetrical and asymmetrical translocations [6].

Our second approach to control the mFISH results looks at single color projections for each fluorescent dye included in the hybridization. As can be seen in Fig. 4, the computer suggested chromosome 14 material (pseudo-color: green) in the middle of the displayed chromosome instead of showing the pseudo-color blue for chromosome 15. This was due to optical and physical properties of the mFISH experiments such as limited resolution and domain overlap. In situations like this, operator intervention is needed to remove ambiguities.

The results of in vitro irradiated lymphocytes (Table 1, Figs. 1–4) show the immense yield of information resulting from mFISH experiments and the characterization of complex aberrations. Keeping in mind that "...it seems no longer possible to consider dicentrics and translocations as the only significant aberrations..." and that "...we need to consider the 'hidden complexity'..." [8], the mFISH approach appears to be a significant step towards a better understanding of radiation-induced chromosome changes. The example in Fig. 5 shows that as many as 15 different chromosomes can be affected by the exposure to 3 Gy of radiation. Such multiply damaged metaphases provide proof for the presence of the suggested 'hidden complexity' [8] which can be expected after irradiation. We found between 3 and 9 chromosomes participating in aberrations in 52.3% of aberrant mitoses. Thus, it seems likely that many radiation induced-aberrations have been overlooked in the past.

The results on hematopoietic colonies, which to the best of our knowledge represents the first application of mFISH to this type of material, showed the

involvement of up to three different chromosomes in clonal aberrations. There is a high likelihood that some of the observed aberrations would have been missed by the two- or three-color WCP approach and that extrapolation would have yielded different results [3–5].

It recently has been proposed that the presence of cells containing clonal aberrations, may have a severe impact on study outcomes when using cytogenetic methods for radiation exposure assessments and that this justifies their careful evaluation [28]. Our preliminary results suggest that mFISH enables one to investigate the clonality of chromosomal aberrations and to proof genomic instability within single colonies.

Furthermore, many cryptic SCAs in cytogenetically normal appearing metaphases, can now be detected and the chromosomes involved can be identified. Nevertheless, it has to be noted that mFISH will not detect all SCAs: small insertions or translocations with a size below the detection limit of mFISH [14] or inversions might be missed.

The idea to apply mFISH for 'biological dosimetry' as it has been done previously with the two- or three-color WCP FISH is quite intriguing. This approach would help to obtain detailed information about SCAs caused by accidental or therapeutic radiation exposure and help to improve biological radiation dose estimates.

Furthermore, mFISH might facilitate the search for a genetic cause of the variation in the response of patient tissue to radiotherapy. Eventually, this could lead to the development of predictive assays for the normal and neoplastic tissue reactions, which might permit to tailor radiotherapy protocols to individual patients [19].

Acknowledgements

This work was supported by the Bundesministerium für Verteidigung, FRG (FV: INSAN I 0697V-3800), by the Commission of the European Communities and by the Ministry for Environment, Nature Conservation and Nuclear Safety, FRG. Partial support of H.-U.G. Weier was provided by the US Army Medical Corps, US Department of Defense, under contract number BC990107 with the E.O. Lawrence Berkeley National Laboratory. We thank Prof. Dr. med. R.U. Peter, Department of Dermatology, University Clinic, Ulm, for providing peripheral blood samples. Furthermore, we acknowledge the help of J. Bode with this paper.

A detailed description of radiation history and clinical syndromes of the Chernobyl accident victim studied in this paper can be obtained from MURAD, Attn.: Prof. Dr. T.M. Fliedner, WHO Collaborating Center for Radiation Accident Management, Helmholtzstr. 20, D-89081 Ulm, FRG.

References

[1] D. Pinkel, T. Straume, J.W. Gray, Cytogenetic analysis using quantitative, high-sensitivity, fluorescence hybridization, PNAS 83 (1986) 2934–2938.

[2] K.L. Johnson, J.D. Tucker, J. Nath, Frequency, distribution and clonality of chromosome damage in human lymphocytes by multi-color FISH, Mutagenesis 13 (3) (1998) 217–227.

[3] J.N. Lucas, A. Awa, T. Straume, M. Poggensee, Y. Kodama, M. Nakano, K. Ohtaki, H.U. Weier, D. Pinkel, J. Gray, G. Littlefield, Rapid translocation frequency analysis in humans decades after exposure to ionizing radiation, Int. J. Radiat. Biol. 62 (1) (1992) 53–63.

[4] S. Knehr, H. Zitzelsberger, H. Braselmann, M. Bauchinger, Analysis for DNA-proportional distribution of radiation-induced chromosome aberrations in various triple combinations of human chromosomes using fluorescence in situ hybridization, Int. J. Radiat. Biol. 65 (6) (1994) 683–690.

[5] E. Gebhart, S. Neubauer, G. Schmitt, S. Birkenhake, J. Dunst, Use of a three color chromosome in situ suppression technique for the detection of past radiation exposure, Radiat. Res. 145 (1996) 47–52.

[6] H.U.G. Weier, N. Lucas, M. Poggensee, R. Segraves, D. Pinkel, J.W. Gray, Two-color hybridization with high complexity chromosome-specific probes and a degenerated alpha-satellite probe DNA allows ambiguous discrimination between symmetrical and asymmetrical translocations, Chromosoma 100 (1991) 371–376.

[7] K. Salassidis, E. Schmid, R.U. Peter, H. Braselmann, M. Bauchinger, Dicentric and translocation analysis for retrospective dose estimation in humans exposed to ionizing radiation during the Chernobyl nuclear power plant accident, Mutat. Res. 311 (1992) 39–48.

[8] J.R.K. Savage, P. Simpson, On the scoring of FISH-'painted' chromosome-type exchange aberrations, Mutat. Res. 307 (1994) 345–353.

[9] J.D. Tucker, W.F. Morgan, A.A. Awa, M. Bauchinger, D. Blakey, M.N. Cornforth, L.G. Littlefield, A.T. Natarajan, C. Shasserre, PAINT: a proposed nomenclature for structural aberrations detected by whole chromosome painting, Mutat. Res. 347 (1995) 21–24.

[10] G.H. Jossart, K.M. Greulich, A.E. Siperstein, Q. Duh, O.H. Clark, H.-U.G. Weier, Molecular and cytogenetic characterization of a t(1;10;21) translocation in the human papillary thyroid cancer cell line TPC-1 expressing the ret/H4 chimeric transcript, Surgery 118 (1995) 1018–1023.

[11] G.H. Jossart, B. O'Brien, J.-F. Cheng, Q. Tong, S.M. Jhiang, Q. Duh, O.H. Clark, H.-U.G. Weier, A novel multicolor hybridization scheme applied to localization of a transcribed sequence (D10S170/H4) and deletion mapping in the thyroid cancer cell line TPC-1, Cytogenet. Cell Genet. 75 (1996) 254–257.

[12] M. Bauchinger, Cytogenetic research after accidental radiation exposure, Stem Cells 13 (1995) 182–190, (Suppl.).

[13] E. Schröck, S. du Manoir, T. Veldman, B. Schoell, J. Wienberg, M.A. Ferguson-Smith, Y. Ning, D.H. Ledbetter, I. Bar-Am, D. Soenksen, Y. Garini, T. Ried, Multicolor spectral karyotyping of human chromosomes, Science 273 (1996) 494–497.

[14] M.R. Speicher, S.G. Ballard, D.C. Ward, Karyotyping human chromosomes by combinatorial multi-fluor FISH, Nat. Genet. 12 (1996) 368–375.

[15] S.X. Shen, Z. Weaver, X. Xu, C. Li, M. Weinstein, L. Chen, X.Y. Guam, T. Ried, C.X. Deng, A target disruption of the murine BRCA1 gene causes gamma-irradiation hypersensitivity and genetic instability, Oncogene 17 (1998) 3115–3124.

[16] H. Zitzelsberger, L. Lehmann, L. Hieber, H.U.G. Weier, C. Janish, J. Fung, T. Negele, F. Spelsberg, E. Lengfelder, E.P. Demidchik, K. Salassidis, A.M. Kellerer, M. Werner, M. Bauchinger, Cytogenetic changes in radiation-induced tumors of the thyroid, Cancer Res. 59 (1999) 135–140.

[17] J. Fung, W. Hyun, P. Dandekar, R.A. Pedersen, H.U.G. Weier, Spectral Imaging in preconception/preimplantation genetic diagnosis (PGD) of aneuploidy: multi-colour, multi-chromosome screening of single cells, J. Ass. Reprod. Genet. 15 (1998) 322–329.

[18] W.G.E. Eisert, M.L. Mendelsohn (Eds.), Biological Dosimetry, Springer-Verlag, Heidelberg, 1985.

[19] A.E. Kiltie, A.J. Ryan, R. Swindell, L.B.P. Barber, C.M.L. West, B. Magee, J.H. Henry, A correlation between residual radiation-induced DNA double-strand breaks in cultured fibroblasts and late radiotherapy reactions in breast cancer patients, Radiother. Oncol. 51 (1999) 55–65.

[20] L.G. Littlefield, L.B. Travis, A.M. Sayer, G.L. Voelz, R.H. Jensen, J.D. Boice Jr., Cumulative genetic damage in hematopoietic stem cells in a patient with a 40-year exposure to alpha particles emitted by thorium dioxide, Radiat. Res. 148 (2) (1997) 135–144.

[21] T. Amenomori, T. Honda, M. Otake, M. Tomonaga, M. Ichimaru, Growth and differentiation of circulating hemopoietic stem cells with atomic bomb irradiation induced chromosome abnormalities, Exp. Hematol. 16 (1988) 849–854.

[22] B.R. Rajendra, I.J. Sciorra, M. Lee, A new and simple technique for chromosomal preparations from peripheral blood lymphocytes, amniotic cell cultures, skin fibroblasts, bone marrow and single cell clones when the yield from harvests are low, Hum. Genet. 55 (1980) 363–366.

[23] I.D. Dubé, C.J. Eaves, D.K. Kalousek, A.C. Eaves, A method for obtaining high quality chromosome preparations from single hemopoietic colonies on a routine basis, Cancer Genet. Cytogenet. 5 (1981) 157–168.

[24] T. Amenomori, M. Tomonaga, T. Matsou, Y. Yoshida, K. Kuriyama, N. Sadamori, M. Ichimaru, A micromethod for chromosome preparation from individual hematopoietic colonies cultured in methylcellulose, Int. J. Cell Cloning 3 (1985) 133–142.

[25] L. Kreja, K.M. Greulich, T.M. Fliedner, B. Heinze, Stable chromosomal aberrations in haemopoietic stem cells in the blood of radiation accident victims, Int. J. Radiat. Biol. 75 (1999) 1241–1250.

[26] D.E. Rooney, B.H. Czepulkowski, Human Chromosome Preparation — Essential Techniques, Wiley, New York, 1997, pp. 50–51; 56–59.

[27] T.M. Fliedner, H. Kindler, D. Densow, A.E. Baranov, A. Guskova, T. Szepesi, The Moscow-Ulm radiation accident clinical history data base, Adv. Biosci. 94 (1994) 271–279.

[28] K.L. Johnson, J. Nath, D.J. Brenner, C.R. Geard, J.D. Tucker, Chromosome aberrations of clonal origin in irradiated and unexposed individuals: assessment and implications, Radiat. Res. 152 (1999) 1–5.

Towards a Full Karyotype Screening of Interphase Cells: 'FISH and Chip' Technology

Heinz-Ulli G. Weier[1], Santiago Munné[2], Robert A. Lersch[1], H.-Ben Hsieh[1], Jan Smida[3], Xiao-Ning Chen[4], Julie R. Korenberg[4], Roger A. Pedersen[5] and Jingly Fung[1,5]

1 Life Sciences Division 74-157, E.O. Lawrence Berkeley National Laboratory, University of California, Berkeley, CA 94720, U.S.A.

2 The Institute for Reproductive Medicine and Science, Saint Barnabas Medical Center, Livingston, NJ 07052, U.S.A.

3 Institute of Radiobiology, GSF-Forschungszentrum für Umwelt und Gesundheit GmbH, D 85758 Oberschleissheim, Germany

4 Medical Genetics Birth Defects Center, University of California, Los Angeles, CA 90048, U.S.A. and

5 Reproductive Genetics Unit, Department of Obstetrics, Gynecology and Reproductive Sciences, University of California, San Francisco, CA 94143-0720, U.S.A.

*To whom correspondence should be addressed.

H.-U. Weier, Department of Subcellular Structure, Life Sciences Division MS 74-157

University of California, E.O. Lawrence Berkeley National Laboratory

1 Cyclotron Road, Berkeley, CA 94720, USA.

Telephone (510) 486 5347, fax (510) 486 5343, email: ugweier@lbl.gov

Summary

Numerical chromosome aberrations are incompatible with normal human development. Our laboratories develop hybridization-based screening tools that generate a maximum of cytogenetic information for each polar body or blastomere analyzed. The methods are developed considering that the abnormality might require preparation of case-specific probes and that only one or two cells will be available for diagnosis, most of which might be in the interphase stage. Furthermore, assay efficiencies have to be high, since there is typically not enough time to repeat an experiment or reconfirm a result prior to fertilization or embryo transfer. Structural alterations are delineated with breakpoint-spanning probes. When screening for numerical abnormalities, we apply a Spectral Imaging-based approach to simultaneously score as many as ten different chromosome types in individual interphase cells. Finally, DNA microarrays are under development to score all of the human chromosomes in a single experiment and to increase the resolution with which micro-deletions can be delineated.

Key Words

cytogenetics, chromosomes, hybridization, FISH, DNA microarrays, digital image analysis (blastomeres)

Introduction

Carriers of balanced translocations have an elevated risk of producing aneuploid germ cells due to disturbed homologue pairing. The resulting partial or total aneusomies lead to spontaneous abortions, stillbirth or severe deficiencies and disease. Assisted reproductive technology now offers couples at risk several diagnostic approaches to reduce the risk of carrying an affected fetus. If the woman carries the abnormality, first polar bodies can be analyzed immediately after oocyte harvest. Following in vitro fertilization, pre-implantation genetic analysis (PGD) can be performed on individual blastomeres biopsied from 3 days old embryos. Since most of the embryonic cells will be found in interphase stage, the diagnostic approach will have to work reliably with either the less condensed chromatin in interphase cell nuclei or the highly condensed DNA in polar bodies (PB's).

Our collaborating laboratories have long been involved in the development of nucleic acid hybridization-based procedures for the rapid detection of structural and numerical chromosome abnormalities. Here, we report the present state of hybridization-based technologies for interphase cell analysis in PGD. Since only one or two cells are available for analysis, our approaches are geared towards obtaining a maximum of cytogenetic information per experiment.

Material and Methods

For more than a decade, our laboratories have been involved in the development of technologies for analysis of interphase and metaphase cells. In collaboration with scientists at the University of California, San Francisco, and the St. Barnabas Medical Center, Livingston, researchers at the E.O. Lawrence Berkeley National Laboratory study the chromosomal composition of blastomeres with regard to numerical as well as structural aberrations. The technical aspects of our probe preparation and multicolor detection protocols have been published previously (Weier et

al., 1994; Jossart et al., 1996; Cassel et al., 1997).

A major goal of our technical developments is to maximize the number of chromosomal targets that can be scored simultaneously. Briefly, probes specific for repeated DNA on chromosomes 15, X, and Y purchased from Vysis (Downers Grove, IL) were labeled with either a green or red fluorochrome (Spectrum Green or Spectrum Orange, respectively). The probes specific for chromosome 9, 13, 14, 16, 18, 21, and 22 were prepared in house and labeled by random priming (BioPrime Kit, GIBCO/LTI, Gaithersburg, MD) incorporating biotin-14-dCTP (part of the BioPrime Kit), digoxigenin-11-dUTP (Roche Molecular Biochemicals, Indianapolis, IN), fluorescein-12-dUTP (Roche Molecular Biochemicals) (Weier et al., 1995), or Cy3-dUTP (Amersham, Arlington Heights, IN). Bound biotinylated probes were detected with avidin-Cy5, and bound digoxigenin-labeled probes were detected with Cy5.5-conjugated antibodies against digoxin (Sigma, St. Louis, MO). Between 0.5 and 3 µl of each probe along with 1 µl human COT1™ DNA (1 mg/ml, GIBCO/LTI) and 1 µl salmon sperm DNA (20 mg/ml, 3'-5', Boulder, CO) were precipitated with 1 µl glycogen (Roche Molecular Biochemicals, 1 mg/ml) and 1/10 volume of 3M sodium acetate in 2 volumes of 2-propanol, air dried and resuspended in 3 µl water, before 7 µl of hybridization master mix [78.6% formamide (FA, GIBCO/LTI), 14.3% dextran sulfate in 2.9x SSC, pH 7.0 (1x SSC is 150 mM NaCl, 15 mM Na citrate)] were added. This gave a total hybridization mixture of 10 µl.

All blastomeres used in the probe developments were obtained from embryos donated by patients enrolled in the IVF Programs of The University of California, San Francisco, or The Institute for Reproductive Medicine and Science of Saint Barnabas Medical Center. In accordance with guidelines set by the internal review boards of these Medical Centers, written consent was obtained from the patients in each case. Embryo biopsies and blastomere fixations

were carried out as described (Munné et al. 1994a, 1996). As indicated below, embryos used for some studies had arrested development or were morphologically abnormal.

Results and Discussion

Traditional filter-based microscope systems limited fluorescence in situ hybridization (FISH) experiments to the simultaneous use of typically no more than 3-5 differently labeled probes for interphase analysis (Munné and Weier, 1996). This is sufficient to detect structural alterations in interphase and metaphase cells or score a few chromosomes in interphase cells (Munné et al., 1994, 1996; Munné and Weier, 1996). We prepared case-specific breakpoint-spanning probe contigs to identify intrachromosomal rearrangements such as inversions or deletions (Cassel et al., 1997). The same approach can be used to demonstrate interchromosomal rearrangements such as reciprocal translocations (Munné et al. 1998a; Weier et al. 1999; Fung et al. 1999). The case-specific probes allow one to discriminate between a normal karyotype, aneuploid cells, and a balanced karyotype carrying the derivative chromosomes. A less time consuming and, thus, less expensive approach using DNA probes that bind distal to the respective breakpoints can only be used to count the number of chromosome copies and thus cannot discriminate between the normal and the balanced karyotypes (Munné et al., 1998b).

Detection of structural chromosome aberrations

Our scheme for the detection of structural alteration is based on the preparation and hybridization of two differently labeled DNA probes that bind on both sides of the respective chromosome breakpoints (Cassel et al., 1996). One probe will be detected in the green fluorescence wavelength interval, while the second probe is made such that it fluoresces red. Normal homologues lack the rearrangement and the probes produce large hybridization domains that appear either red or green in the fluorescence microscope. At the same time, we counterstain the

DNA with 4, 6-diamino-2-phenylindole (DAPI) which fluoresces blue under ultraviolet light excitation. If the cell contains a derivative chromosome, the hybridization result will show a red/green associated or partially overlapping signal indicative of the translocation event. Thus, we detect structural alteration and score homologues at the same time.

Our work is greatly facilitated by access to resources created in the course of the International Human Genome Sequencing Project, such as large insert genomic DNA libraries (bacterial or yeast artificial chromosomes (BACs or YACs, respectively), high resolution physical maps or collections of cytogenetically mapped DNA probes (Kim et al., 1996; Chen et al., 1996; Korenberg et al., 1999). This enables us to prepare case-specific probe sets suitable for interphase cell analyses of most patient cells within a few weeks. Once optimized, these probe sets allow to rapidly determine the exact number of normal chromosomes and derivative chromosomes in somatic cells from translocation carriers as well as their germ cells or offspring. So far, however, these procedures failed to produce the desired increase in pregnancy rates in cases where one spouse carried a balanced reciprocal translocation. Our concern is that the impaired homologue pairing in the carriers leads to gain or loss of other chromosomes which remains undetected in assays scoring only the translocation chromosomes.

The recent introduction of Spectral Imaging (SIm) now allows one to interrogate a much larger number of targets, thus producing a more comprehensive picture of the chromosomal composition of the cells. SIm allows an investigator to discriminate an increased number of fluorescent probes by exciting fluorescent molecules over a broad spectral range and by recording the fluorescence emission spectral using an interferometer.

Detection of numerical chromosome abnormalities using Spectral Imaging (SIm)

Chromosome abnormalities occur with astonishing frequency in humans, being present in an estimated 10-30% of all fertilized eggs. Over 25% of all the miscarriages are monosomic or

trisomics, making aneuploidy the leading known cause of pregnancy loss. Ideally, one likes to detect aneuploidy involving any of the 24 human chromosomes for preimplanation genetic diagnosis and prenatal diagnosis. Thus, an analytical method to enumerate as many chromosomes as possible in few interphase cells is highly desirable. Using a set comprised of seven chromosome–specific probes (chromosome 10, 14, 16, 18, 22, X and Y) hybridized to lymphocyte interphase nuclei, we demonstrated that Spectral Imaging system provides a significant improvement over conventional filter-base microscope systems for enumeration of multiple chromosomes in interphase nuclei (Fung et al., 1998).

Using mostly yeast or bacterial artificial chromosome probes for cytogenetic analyses of blastomeres and detection of structural alterations, we are building panels of probes to simultaneously score 10 or more different chromosomes. Further increases in the number of probes is complicated due to occasional overlap of chromosome domains or local variation in hybridization efficiency. We developed a 10-chromosomes probe set (chromosomes 9, 13, 14, 15, 16, 18, 21, 22, X, and Y) for the purpose of labeling DNA targets most frequently associated with aneuploidy and spontaneous abortions and tested its application in PGD (blastomeres from abnormal human preimplantation embryos) and prenatal diagnosis (uncultured amniocytes obtained by amniocentesis). Results demonstrated increasing levels of background fluorescence on different cells after hybridization in the order: (uncultured amniocytes) >> (blastomeres) > (interphase cells from lymphocytes). All blastomeres fixed for this study (N=25) spread very well. Fourteen nuclei (56%) showed interpretable hybridization results, and most of them were karyotyped as abnormal, since all those cells were from 1PN and 3 PN human embryos, and had arrested development or were morphologically abnormal. The signals from 11 nuclei (44%) were faint. This may be related to the quality of the embryos, since all of them were developing

abnormally. The fixation of uncultured amniocytes on slides for Spectral Imaging analysis turned out to be somewhat difficult. Most nuclei were not flattened out, presenting a problem due to the limited focal depth. Overlapping signal domains were a problem in uncultured amniocytes, where only about 20% of all cells showed interpretable spreads. In summary, Spectral Imaging has demonstrated advantages for evaluating numerical chromosomal abnormalies in single interphase cells. Its utility for chromosome scoring, however, remains limited due to chromosome domain overlap.

DNA microarrays (Chips)

The DNA microarrays represent an exciting new technology with applications ranging from gene expression profiling to determination of gene copy number changes in tumors. We are presently investigating this approach in which the DNA probes are immobilized on glass slides as a strategy complementing FISH studies. The DNA from the embryonic cells is labeled in one color (e.g. red), while an equal amount of a reference DNA probe is labeled in a different color (e.g. green). These differentially labeled DNA are combined, denatured and hybridized to a DNA micro-array or "chip" in a quantitative manner. Results are obtained after reading the micro-arrays with specially designed fluorescence scanners as red/green or red/infrared fluorescence ratios. After normalization, every increase or decrease from the average ratio indicates an abnormal number of copies of the hybridization target.

In practice, the DNA contained in a single cell is not sufficient to generate measurable signals. The commonly used protocols therefore include a DNA in vitro amplification step using a random primer or oligonucleotide with arbitrary sequence prior to labelling. The DNA to be immobilized can be obtained by standard isolation protocols or by in vitro DNA amplification. We use a DNA spotter based on the design published by P. Brown's group at Stanford

University (Scheena et al., 1996). This allows us to spot small amounts of DNA on poly-L-lysine coated glass slides with a 100-200 micron pitch. A 288-spot DNA micro-array like the test array depicted schematically in Fig. 1 then measures no more than a few square millimeters. This small size of micro-arrays is an advantage over larger arrays prepared on nylon filters, because it requires less amount of labeled DNA sample in the hybridization reaction.

We are presently preparing DNA test chips to develop the methods and study parameters such as probe preparation, hybridization conditions and chip reader performance. Our long term objective is the development of reliable procedures to detect structural as well as numerical abnormalities using a combination of 'FISH and chip' technology. Chips to be used in those studies will carry several hybridization targets per chromosome arm, thus allowing a more detailed gene dosage determination or delineation of full or partial aneusomies than the FISH-based assays.

Acknowledgments

The authors gratefully acknowledge support from Dr. J. Cohen. We also wish to thank M. Cassel, J. Garcia, J. Wu and C. Marquez for skillful assistance and all anonymous patients who made this study possible by donating embryos. R.A.L., J.S. and H.B.H. were supported in part by a grant from the University of California (U.C.) Systemwide Biotechnology Research and Education Program (to H.U.W.). Additional salary support for H.B.H. was provided by the Cancer Research Foundation of America. We acknowledge the support from the U.S. Dept. of Defense, U.S. Army Medical Research and Material Command (BC980937). J.F. was supported in part by an NIEHS training grant (5-T32-ES07106-17).

References

Cassel, M.J., Munné, S., Fung, J., Weier, H.U.G., 1997. Carrier-specific breakpoint-spanning DNA probes: an approach to pre-implantation genetic diagnosis [PGD] in interphase cells. Human Reprod 12, 101-109.

Chen, X-N., Mitchell, S. Sun, ZG., Noya, D., Ma, S., Sekhon, G. S., Thompson, K., Hsu, W-T., Wong, P., Wang, N., Shcreck, R., Falk, R., Korenberg J. R., 1996. The Integrated BAC Resource: a powerful new molecular tool for prenatal genetics. Am. J. Hum. Genet. 59:A12.

Fung, J., Munné, S., Duell, T., Weier, H.-U.G., 1998a. Rapid cloning of translocation breakpoints: from blood to YAC in 50 Days. J. Biochem. Mol. Biol. Biophys. 1, 181-192.

Fung, J., Hyun, W., Dandekar, P., Pedersen, R.A., Weier, H.-U.G., 1998b. Spectral Imaging in Preconception/Preimplantation Genetic Diagnosis (PGD) of Aneuploidy: Multi-Colour, Multi-Chromosome Screening of Single Cells. J Ass Reprod Genet 15, 322-329.

Fung, J., Munné, J., Garcia, J., Kim, U.-J., Weier, H.-U.G., 1999. Reciprocal translocations and infertility: molecular cloning of breakpoints in a case of constitutional translocation t(11;22)(q23;q11) and preparation of probes for preimplantation genetic diagnosis (PGD). Reprod. Fert. Devel. 11, 17-23.

Jossart, G.H., O'Brien, B., Cheng, J.-F., Tong, Q., Jhiang, S. M., Duh, Q., Clark, O. H., Weier H.-U.G., 1996. A novel multicolor hybridization scheme applied to localization of a transcribed sequence (D10S170/H4) and deletion mapping in the thyroid cancer cell line TPC-1. Cytogenet. Cell. Genet. 75, 254-257.

Kim, U. J., Shizuya, H., Kang, H. L., Choi, S. S., Garrett, C. L., Smink, L. J., Birren, B. W., Korenberg, J. R., Dunham, I., Simon, M. I., 1996. A bacterial artificial chromosome-based framework contig map of human chromosome 22q. Proc. Natl. Acad. Sci. USA 93, 6297-300.

Korenberg J. R., Chen, X-N., Sun, Z, Shi, Z-Y., Shi, Ma, S., Vataru, E., Yimlamai, D. Weissenbach, J. S. Shizuya, H., Melvin, S. I., Gerety, S. S., Nguyen, H., Zemsteva, I. S. Hui, L., Silva, J. Wu, X., Birren, B.W., Hudson, T. J., 1999. Human Genome Anatomy: BACs integrating the genetic and cytogenetic maps for bridging genome and biomedicine. Genome Res. 9, 994-1001

Munné, S. , Grifo, J., Cohen, J., Weier, H.-U. G., 1994. Mosaicism and aneuploidy in arrested human preimplantation embryos: a multiple probe fluorescence in situ hybridization (FISH) study. Am. J. Hum. Genet. 55, 150-159.

Munné, S., Dailey, T., Finkelstein, M., Weier, H.U.G., 1996. Reduction in overlaps and missing signals in interphase-FISH. J. Assist. Reprod. Genet. 13,149-156.

Munné S., Weier H.-U.G., 1996. Simultaneous enumeration of chromosomes X,Y,18,13, and 21 in interphase cells for preimplantation genetic diagnosis of aneuploidy. Cytogenet. Cell. Genet. 75, 264-270.

Munné, S., Fung, J., Cassel, M.J., Márquez, C., Weier, H.-U.G., 1998a. Preimplantation genetic analysis of translocations: case-specific probes for interphase cell analysis. Human Genet. 102, 663-674

Munné, S., Morrison, L., Fung, J., Márquez, C., Weier, U., Bahçe, M., Sable, D., Grundfelt, L., Schoolcraft, B., Scott, R., Cohen, J., 1998b. Spontaneous abortions are significantly reduced after pre-conception genetic diagnosis of translocations. J. Ass. Reprod. Genet. 15, 290-296.

Schena, M., Shalon, D., Heller, R.. Chai, A., Brown, P.O., Davis, R.W., 1996. Parallel human genome analysis: microarray-based expression monitoring of 1000 genes. Proc. Natl. Acad. Sci. U.S.A. 93, 10614-10619.

Weier, H.-U., Rosette, C.D., Matsuta, M., Zitzelsberger, H., Matsuta, M., Gray, J., 1994. Generation of highly specific DNA hybridization probes for chromosome enumeration in human interphase cell nuclei: isolation and enzymatic synthesis of alpha satellite DNA probes for chromosome 10 by primer directed DNA amplification. Meth. Mol. Cell. Biol. 4, 231-248.

Weier, H.-U. G., Wang, M., Mullikin, J. C., Zhu, Y., Cheng, J. F., Greulich, K. M., Bensimon, A., Gray, J. W., 1995. Quantitative DNA fiber mapping. Hum. Mol. Genet. 4, 1903-1910.

Weier, H.-U.G., Munné S., Fung J., 1999. Patient-specific probes for preimplantation genetic diagnosis (PGD) of structural and numerical aberrations in interphase cells. J. Assist Reprod Genet. 16, 182-189.

Figure Legend

Figure 1. Prototype DNA microarray for technology development. The chip contains from left to right: control DNA spots (6 samples), PCR amplified YAC DNA (12 clones), BAC array 1 (46 clones for copy number determination in breast cancer research), cDNA (62 tyrosine kinase cDNA for expression profiling), and BAC array 2 (24 clones for chromosome enumeration in PGD). All samples are spotted in duplicate. The total number of DNA spots of 300 arrayed with a 180 micrometer pitch leads to array dimensions of 2.08 mm x 4.42 mm. Each slide contains 2 identical microarrays.

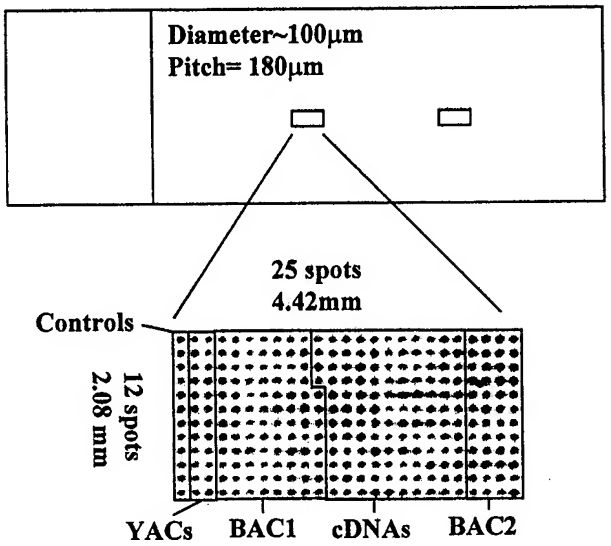
Diameter~100μm
Pitch= 180μm
25 spots
4.42mm
Controls
12 spots
2.08 mm
YACs
BAC1
cDNAs
BAC2

The Growth and Metastasis of Human, HER-2/neu-Overexpressing Tumor Cell Lines in SCID Mice

Running Title: HER-2-Overexpressing Tumors in SCID Mice

Birgitta Clinchy[1], Adi Gazdar[2], Rosalia Rabinovsky[1], Eitan Yefenof [1,3], Brian Gordon[4], and Ellen S. Vitetta[1,4]

[1]Cancer Immunobiology Center and [2]Department of Pathology, University of Texas Southwestern Medical Center at Dallas, 5323 Harry Hines Boulevard, Dallas, Texas 75235-8576, USA, [3]Hadassah Medical School, Jerusalem, Israel, [4]Carolinas Medical Center, 1000 Blythe Boulevard, Charlotte, North Carolina, 28203.

[5]To whom correspondence and reprint requests should be sent:
Cancer Immunobiology Center
University of Texas Southwestern Medical Center at Dallas
5323 Harry Hines Boulevard
Dallas, Texas 75235-8576
Telephone: 214-648-1200
Fax: 214-648-1204

Current addresses:
Dr. Birgitta Clinchy, The University Hospital, Tumor Immunology, 581 85 Linkoping, Sweden
Ms. Rosalia Rabinovsky, Hadassah Medical School, P.O. Box 12272, Jerusalem 91020, Israel

Summary

HER-2/neu is overexpressed on a variety of human adenocarcinomas and overexpression has been associated with a poor prognosis. For this reason, HER-2 has become an attractive target for immunotherapy. To facilitate testing of anti-HER-2-monoclonal antibodies (MAbs) and immunotoxins (ITs), we have evaluated the *in vivo* growth and metastatic spread of three HER-2 overexpressing human breast cancer cell lines (BT474, MDA-MB-453 and HCC1954) and one ovarian cancer cell line (SKOV3.ip1) in pre-irradiated male SCID mice using subcutaneous (s.c.), intravenous (i.v.) and intraperitoneal (i.p.) routes of injection. All the cell lines tested grew as s.c. tumors and the growth of BT474 and MDA-MB-453 cells after s.c. injection was improved by co-inoculation with Matrigel. Metastases to the lungs were detectable by PCR or histopathology after s.c. injection of BT474 and to a much lesser extent after s.c. injection of HCC1954, MD-MB-453 and SKOV3.ip1cells. I.P. injection of HCC1954 and SKOV3.ip1 cells produced fatal ascites while i.v. injection of SKOV3.ip1, but not BT474 or MDA-MB-453 cells, resulted in infiltration of lungs and death within 9-11 weeks.

Key words: breast cancer, *in vivo* tumor models, Her-2/neu, Metastasis, SCID mice, soluble Her-2.

Introduction

The human homologue of the rat neu oncogene (HER-2, erbB-2) belongs to the EGF receptor family (1). The HER-2 protein product (p185) is overexpressed on 30% of all breast cancers (2) and there is considerable evidence that the overexpression of HER-2/neu is associated with a highly malignant tumor phenotype since transfection of the HER-2 gene into HER-2^- tumor cells leads to an increase in both metastatic behavior and aggressive *in vivo* growth (3,4). Accordingly, overexpression of HER-2 on tumors from breast cancer patients correlates with a shorter time to relapse and decreased survival (5). Since HER-2 is expressed at lower (normal) levels in many normal tissues (6), it makes an attractive target for immunotherapy. Some monoclonal antibodies (MAbs) raised against HER-2 inhibit the *in vitro* and *in vivo* growth of HER-2 overexpressing cells (7). Anti-HER-2 immunotoxins (ITs) and radioimmunoconjugates also show efficacy both *in vitro* and *in vivo* in animal xenograft models (7,8). The humanized anti-HER-2 MAb, 4D5 (Herceptin™), has been approved by the FDA and has demonstrated increased survival of relapsed patients with HER-2-overexpressing tumors (9).

Despite the documented aggressive behavior of HER-2^+ breast cancer tumors, few *in vivo* models of xenografted HER-2-overexpressing breast cancers have been described (see Table 3). Hence, HER-2-based therapeutics are usually tested *in vivo* on tumor cell lines transfected with the gene for HER-2 (10-12) or on naturally HER-2-overexpressing cancer cell lines of other origin, like the ovarian cell line SKOV3 (10,13). We wished to develop an *in vivo* model for testing MAb-based anti-HER-2 therapy on naturally HER-2 overexpressing human breast cancer in a setting of minimal residual disease (MRD). Thus, in an animal model with localized tumor

growth that metastasizes to distal sites, the local tumor could be surgically removed and/or treated with chemotherapy or radiation and the metastases then treated with immunotherapy.

Our results suggest the BT474 cell line metastasizes to lungs and kidneys in pre-irradiated SCID mice. Furthermore, levels of sHER-2 in the sera parallel tumor growth after s.c. injection. This will provide a useful model in which to further address the efficacy of MAb constructs in treating metastatic minimal residual disease.

Materials and Methods

Mice

Male CB.17-SCID/SCID mice, originally from Dr. Bosma's colony at Fox Chase Cancer Center were bred at the Carolinas Medical Center. The use of animals in this study was approved by the UT Southwestern Medical Center Institutional Animal Care and Use Committee, based on compliance with NIH guidelines for the care and use of laboratory animals. Mice were housed in a pathogen-free facility without prophylactic antibiotics. Sera were screened by ELISA for the presence of mouse immunoglobulin (Ig) and mice with serum levels exceeding 10 ug/ml were considered leaky and were not used (14). All manipulations were performed in a laminar flow hood.

Cell lines

The human breast cancer cell lines BT474 (15), MDA-MB-453 and MDA-MB-435 (16) were kindly provided by Dr. J. Price, M.D. Anderson Cancer Center, Houston. The breast cancer cell line, HCC1954, was recently established from a ductal carcinoma by Gazdar et al (17). SKOV3.ip1 is a variant of the ovarian cancer cell line SKOV3 with higher HER-2 expression, isolated from the ascites of a SCID mouse (18). All cell lines were maintained as monolayer cultures in minimum essential medium (MEM, GIBCO BRL, Grand Island, NY) supplemented with 1% vitamins for MEM, 2mM L-glutamine, 0.1 mM non-essential amino acids, 1 mM sodium pyruvate, 1% Hepes buffer (all from GIBCO) and 10% heat-inactivated fetal calf serum (FCS, Hyclone, Logan, Utah). Cultures were grown in 37°C at 5% CO_2 and cells were passaged either every four days or when 70% confluent. Prior to passage, cells were removed from the flasks with trypsin/EDTA and washed (GIBCO BRL). All cell lines were free of mycoplasma.

Collection of culture supernatants (SNs) from tumor cell lines

SNs were prepared by seeding $1x10^6$ tumor cells in 25 cm^2 tissue culture flasks (Falcon /Becton Dickinson Labware, Lincoln Park, NJ) in 4 ml of medium. SNs were collected after 5 days. Cells were removed by centrifugation at 2000 RPM after which the SNs were filtered through a 0.22 um filter and stored at -20° C.

MAbs

The mouse anti-HER-2 MAbs used in this study were generated in our laboratory by immunizing mice with the extracellular domain of human Her-2 and screening the MAbs on both plate-bound HER-2 and HER-2^+ cells. HER50, HER66 and HER81 are $IgG_1\kappa$s which recognize three different epitopes on the extracellular domain of HER-2 (as determined by crossblocking experiments). None of the MAbs recognizes the EGFR, HER-3 or HER-4. MAbs were purified by affinity chromatography of hybridoma culture SNs on Sepharose protein G (Pharmacia, Piscataway, NJ).

Flow cytometry

Immunofluoresent staining of tumor cells was carried out using the anti-HER2 MAb, HER81. $1x10^6$ unfixed, trypsinized cells, suspended in PBS with 5% normal rat serum (NRS, Cappel Research Products, Durham, NC), were incubated on ice for 20 min with 1 ug of HER81 or an isotype matched control MAb (MOPC-21). Cells were then washed twice with cold PBS and incubated on ice for 20 minutes with a 1/500 dilution of FITC-conjugated goat anti-mouse IgG (GAMIg) absorbed with human serum (Sigma Immunochemicals, St.Louis. IL). Cells were

washed, fixed in 1% paraformaldehyde and maintained at 4° C until they were analyzed on an Epics-profile II (Coulter Co, Hialeah, FL).

Injection of tumor cell lines

Cells were harvested after treatment for two minute with 0.05% Trypsin/EDTA followed by one wash in medium and two washes in Hank's balanced salt solution (HBSS, GIBCO). Cell viability was determined by trypan blue dye exclusion and cell numbers were determined using a hemocytometer. In some experiments, cells were mixed with an equal volume (100 ul) of ice cold Matrigel (Becton Dickinson). The original formulation of Matrigel matrix containing phenol red was used. 2×10^6 cells in 100 ul HBSS were injected into SCID mice (irradiated 24 hours previously with 150 cGy) either i.p., s.c. on the lateral flank, or i.v. via the tail vein.

Measurement of tumor volume

The diameter of s.c. tumors were measured once a week using venier calipers. The volume was calculated according to a published formula; $mm^3 = \text{length} \times (\text{width})^2 \times ½$ (19).

Polymerase chain reaction (PCR)

DNA was extracted from dissected organs using the QIAmp tissue DNA purification kit from Qiagen Inc., Chatsworth, CA, following the manufacturer's recommended protocol. DNA samples were stored at -20°C until further use. Human DNA was detected by PCR amplification of a 300 base pair fragment using primer pairs for specific for the human RNA polymerase II gene, as previously described by Bai et al. (20). The primer pairs were 5'-GCATCAAATACCCAGAGACG-3' and 3'-CCACGTGAAACACAGGCTTG-5'.

Amplification reactions in the presence of 2.5 units Taq DNA polymerase (Promega, Madison, WI), were carried out at 95°C for two minutes followed by 34 cycles of 94°C for 0.5 minutes, 60°C for 0.5 minutes and 72°C for one minute in a Perkin-Elmer DNA thermal cycler 480. A final extension at 72°C for 10 minutes was added after the 34 cycles. The PCR-amplified product was electrophoresed in 2% agarose gels and the DNA was visualized by ethidium bromide staining and UV transillumination. DNA from 10 human breast cancer cells mixed with 100 ng SCID mouse DNA (equivalent to $1x10^5$ cells) could be detected in this assay (data not shown).

Peritoneal lavage

The perioneal cavities of SCID mice injected i.p. 10 weeks earlier with HCC1954 cells were flushed once with 3-5 ml of HBSS containing 5% FCS. Recovered cells were resuspended using a syringe and a 21gauge needle followed by filtration through a nylon mesh. Cells were analyzed by flow cytometry the same day. Other lavage samples were placed in tissue culture flasks without further cell suspension and were photographed using an Olympus SC35 camera mounted on an inverted Olympus CK2 microscope.

Immunohistochemistry

Mouse tissues were fixed in 10% buffered formalin for at least 24 hours and then mounted in paraffin. Immunohistochemical staining was performed by the UT Southwestern Pathology Immunohistochemistry Laboratory using a BioTek Solutions TechMate^{tm} 1000 automated immunostainer (Ventana Bio Tek Systems, Tucson, AZ). 3 um paraffin sections were immunostained with affinity-purified rabbit anti-human c-erbB-2 (Dako Co, Carpinteria, CA)

followed by biotinylated goat anti-rabbit Ig. Positive reactions (dark brown) were visualized by horseradish peroxidase-conjugated Streptavidin-biotin complex and diaminobenzidine (DAB). Sections were counterstained with hematoxylin.

Levels of soluble HER-2 (sHER-2) in blood or tissue culture supernatants (SNs)

200 uls of blood were collected from the tails of tumor-bearing SCID mice and levels of sHER-2 were measured using an ELISA with either a commercially available ELISA kit from Oncogene Research Products (Calbiochem, Cambridge, MA) or a sandwich ELISA developed with our own anti-HER-2 MAbs. For the latter, 96-well ELISA plates (Corning) were coated with 1.5 ug/well of the mouse anti-human HER-2 MAb, HER50, overnight at 4°C. Dilutions of culture SNs or serum samples in PBS/0.1% bovine serum albumin (BSA) were added and incubated at room temperature for 2 hours. Plates were overlayed with 1.9 ug/ well of biotin-conjugated HER66 and incubated overnight at 4°C. The plates were then washed four times with PBS/0.02% Tween. A 1/10,000 dilution of alkaline phosphatase-conjugated extravedin (Biosource) was added. After incubation at room temperature for two hours, cells were washed four times. The amount of bound secondary antibody was measured by the hydrolysis of paranitrophenyl phophate substrate (Sigma Chemical Co) at 405 nm in a Thermomax microplate reader (Molecular devices Co., Menlo Park, CA). The amount of sHER-2 was extrapolated from the HER-2 (p185, Oncogene Research Products) standard curve and expressed as units. The limit of detection of this assay was 45 U of sHER-2/ml.

Results

Surface expression of HER-2 on tumor cell lines

Four tumor cell lines that overexpressed HER-2 were selected for this study. In accord with previous reports (17,21) (18), high levels of membrane HER-2 could be detected with MAb HER81 on the breast cancer cell lines BT474, HCC1954 and the ovarian tumor cell linesSKOV3.ip1 while intermediate levels of HER-2 were expressed on the breast cancer cell line MDA-MB-453 (data not shown).

In vivo growth of tumor cell lines in SCID mice

In order to evaluate the *in vivo* growth of these cell lines in SCID mice, 1-2 x 10^6 suspended cells were inoculated into pre-irradiated male SCID mice. Different routes of injection were evaluated [s.c. ± basement membrane matrix (Matrigel), i.p. and i.v.]. The mice were followed for up to 16 weeks. The take rate for each cell line is described in Table 1.

i. <u>s.c. inoculation</u>.

All cell lines formed s.c. tumors when injected on the lateral flank. Tumor volumes after s.c. injection with or without Matrigel are shown in Figure 2. BT474, HCC1954 and MDA-MD-453 formed s.c. tumors considerably more slowly than SKOV3.ip1. Both BT474 and MDA-MB-453 had improved take rates and grew more rapidly if the tumor cells were co-injected with Matrigel (Table 1 and Figure 2). HCC1954 s.c. tumors varied considerably in size between individual mice. These tumors often developed necrotic areas that were shed, while the underlying tumor tissue continued to grow. This was the case both for HCC1954 tumors co-injected with Matrigel and for tumors injected without Matrigel.

ii. i.p. inoculation.

As described (18), the ovarian cell line SKOV3. ip1 grew very aggressively after i.p. injection resulting in death of the animals within 4-5 weeks. Likewise, SCID mice injected with $1x10^6$ HCC1954 cells i.p. developed fatal ascites with liver and kidney infiltration within 8-15 weeks. Autopsy revealed large plaques of tumor cells growing on the peritoneal wall. Cells recovered through peritoneal lavage were organized in three dimensional structures resembling mammary ducts (Figure 3A). These cells retained strong HER-2 expression, as determined by flow cytometry (Figure 3B). When the peritoneal lavage cells were returned to tissue culture, the cells again grew as adherent monolayers and the three dimensional structure was lost. Furthermore, we observed modest ascites in 2 out of 5 SCID mice inoculated i.p. with MDA-MB-453, whereas there was no evidence of ascites growth of BT474 after i.p. injection into 10 mice (with the exception of one mouse were tumor growth in the kidney was detected by PCR).

iii. i.v. inoculation.

I.V. inoculation of HCC1954 was not studied since it led to immediate death of the mice due to the formation of emboli. This could not be avoided by injecting fewer cells, re-suspending the cells, or filtering the cells. SKOV3.ip1 cells rapidly infiltrated the lungs after i.v. injection and death of the mice occurred within 9-11weeks. At this time, large macroscopic tumors were observed in the lungs. However, no infiltration of spleen, liver, kidney, pancreas, testis or bone marrow could be detected, neither by histopathology nor by PCR. In the case of i.v. injected BT474 cells, no tumor cells were found in the lungs, but one of five mice examined had PCR-

detectable tumor cells in kidney, pancreas and testes. There was no evidence of tumor growth after i.v. inoculation of MDA-MB-453 cells.

Metastatic Growth

All surviving mice were sacrificed at 15-16 weeks and necropsied. Major organs, bone marrow (BM) and blood were collected and either preserved in 10 % buffered formalin for histopathology or frozen for later PCR evaluation. The metastatic growth of the tumor cell lines was evaluated by histopathology and/or by PCR amplification of a sequence of the human RNA polymerase gene (Figure 4). A 300 bp fragment was amplified in DNA from SCID mouse tissue containing human tumor cells but not in DNA from normal SCID mice (data not shown). Metastatic lesions, observed by histopathology, were usually very small and rarely consisted of more than approximately 10 cells with only one or two foci per section. A summary of metastastatic growth by the different cell lines is shown in Figure 5.

In all cases of s.c. tumors, metastases were only found when the s.c. tumor had a volume larger than 800 mm^3. Of all the cell lines injected s.c., BT474 metastasized most frequently and metastases could be detected both by histopathology and by PCR . Only one case of PCR amplification of human RNApolymerase in BM could be found (HCC1954 injected s.c.) among 60 examined mice.

In some mice metastases were also observed in lungs and kidney after i.p. injection. In two of five mice injected i.p. with MDA-MB-453 tumors acscites development was evident and tumors could also be detected in lung by PCR. However, tumor growth in the lungs could not be

confirmed by histopathology. Lungs from five mice with massive growth of HCC1954 cells in the peritoneum were examined by PCR. In two of these human RNApolymerase was amplified. Again, these results could not be verified by histopathology. Multiple organs in the peritoneum as well as lungs were examined by PCR in mice injected i.p. with BT474 cells. Only one case of PCR amplification could be found and this occurred in the kidney. In mice injected with SKOV3.ip1, metastatic growth outside the peritoneal cavity was not evident based on gross pathology. Metastases to lungs or BM in these mice were not examined by PCR or histopathology since SKOV3.ip1 has already been reported not to metastasize from the peritoneum (18).

As already mentioned, i.v. injection resulted in macroscopic lung tumors in mice injected with SKOV3.ip1. however, using PCR or histopathology, we could not identify tumors cells in other organs or in the BM of these mice, nor did we find evidence of tumor growth in any organ in mice injected i.v. with MDA-MB-453 or BT474 (with the exception of one mouse).

Surface expression of HER-2 on metastatic BT474 cells

Immunohistochemistry was performed on paraffin embedded lung tissue from SCID mice injected s.c with BT474 tumor cells suspended in Matrigel to verify that the xenografted tumors still expressed HER-2 after growth *in vivo*. As shown in Figure 6, HER-2 expression was preserved in BT474 cells which had metastasized from the s.c. site to the lung.

Release of sHER-2 into the serum of tumor-bearing SCID mice

Previous reports have shown that the extracellular portion of HER-2 can be shed from the surface of HER-2 overexpressing tumors (22) and that soluble HER-2 (sHER-2) can be detected in the sera of tumor-bearing mice (23,24). To verify that the HER-2^+ tumor cell lines released HER-2, cell-free culture SNs from confluent tumor cell cultures were assayed for the presence of sHER-2 by ELISA. As shown in Table 2, all the HER-2-overexpressing tumors released large amounts of sHER-2 into the culture medium, whereas no sHER-2 could be detected in SNs from the HER-2^- MDA-MB-435 cell line. Intermediate levels of sHER-2 was detected in culture SNs from MDA-MB-453 cells, which express less surface HER-2 as compared to BT474, HCC1954 and SKOV3. ip1 {24895 and Figure 1).

To determine whether the growth of the HER-2^+ tumors in SCID mice was accompanied by increased serum levels of sHER-2, sera collected at the time of death were also assayed for sHER-2s. As can be seen in Figure 7, virtually all SCID mice with s.c. tumors had detectable levels of sHER-2 in their sera at the time of death and the levels of sHER-2 correlated with the s.c. tumor burden. Likewise, growth of SKOV3 ip.1 tumors, following i.v. injection, resulted in high levels of sHER-2 in sera (Table 2). Peritoneal growth of HCC1954 also resulted in very high levels of sHER-2. Furthermore, two out of five SCID mice inoculated i.p. with MDA-MB-453 had detectable serum levels of sHER-2 at the time of death (Table 2). These mice had modest ascites formation and tumor cells were also detected in lungs by PCR. No sHER-2 was detected in the sera of SCID mice injected i.p. or i.v. with BT474 tumor cells or i.v. with MDA-

MB-453 cells (Table 2). sHER-2 could not be detected in sera from normal SCID mice or from SCID mice carrying large (> 1000 mm3) MDA-MB-435 s.c. xenografts (data not shown).

Discussion

We have developed a panel of apoptosis-inducing HER-2 MAbs several of which also make potent immunotoxins when conjugated to ricin toxin A-chain (RTA). In order to test these reagents *in vivo*, it would be highly desirable to have a mouse xenograft model in which human HER-2-overexpressing breast tumors would grow locally and predictably metastasize. In such a model, one could then surgically remove or conventionally treat the primary tumor and evaluate the efficacy of these reagents on the residual metastatic disease. Unfortunately, there are only a few *in vivo* models of HER-2-overexpressing human breast tumors in mice and metastatic growth of these tumors has only been partly evaluated (Summarized in Table 3). A number of HER-2-non-overexpressing breast cancer cell lines have been found to metastatize *in vivo* {25049}(25-28) but these are not suitable for anti-HER-2 MAb therapy. For this reason, naturally HER-2- overexpressing ovarian and gastric cancer cell lines (10-12) or HER-2 transfected NIH3T3 fibroblasts (10,29-31) have instead been utilized.

The objective of this study was to develop a more useful *in vivo* model of metastatic HER-2-overexpressing breast tumors. The major findings to emerge from this study are as follows: 1. Three HER-2 overexpressing breast cell lines, BT474, MDA-MB-453 and HCC1954, as well as the ovarian cancer cell line SKOV3.ip1 grew as s.c. tumors; the SKOV3.ip1 tumors grew most rapidly. Co-injection of Matrigel enhanced the s.c. growth of BT474 and MDA-MB-453 tumors but not HCC1954 tumors. Matrigel did, however, improve the rate of take of the HCC1954, BT474 and MDA-MB-453 cell lines. 2. After s.c. injection of BT474, the cells routinely metastasized to the lung and occasionally to the kidney. However, in contrast to a previous report (32), BT474 did not metastasize to lymph nodes in our studies. In some cases, lung

metastases were observed after s.c. injection of HCC1954 and MDA-MB-453 cells. Metastatic spread to the bone marrow was only found in one mouse injected s.c. with HCC1954. 3. After i.v injection, SKOV3.ip1 grew in the lung, but BT474 and MDA-MB-453 did not. 4. HCC1954 grew aggressively in all mice after i.p. injection, but spread to the lung in only 40% of the mice. HCC1954 formed ductal shapes in the peritoneum after i.p. injection but these structures could not be maintained *in vitro*. 5. sHER-2 could be detected in sera from all mice injected s.c. with tumor cells and the levels correlated with the tumor burden as well as with the level of overexpression of HER-2 on the particular tumor cells used. Taken together these findings suggest that the BT474 cell line best satisfies the criteria of a localized HER-2-overexpressing tumor which predictably metastasizes and where HER-2 expression is maintained.

The *in vivo* growth of BT474 after s.c. inoculation has been reported in both nude and beige/nude/xid mice with metastases in lymph nodes and lungs (Table 3). However, estrogen supplementation was required to achieve consistent tumor growth (32,33). Since it has been shown that estrogen can modulate HER-2 expression (34,35) it would be preferable to have an *in vivo* model where the use of estrogen would not be required. In nude mice, BT474 grew without estrogen after orthotopic injection with Matrigel into the mammary fat pads (mfp) (36), but metastatic spread was not evaluated. We used male SCID mice and we observed a 100% take rate without estrogen supplementation when the BT474 cells were co-inoculated s.c. with Matrigel. Several reports have indicated that SCID mice may be better suited for xenografting than nude mice with regard to both a higher take rate and more routine metastatic growth (37-39). In addition, breast cancer xenografts metastasized more readily to lungs in SCID mice compared to bg-nu-xid and nude mice (36). Furthermore, sub-lethal whole-body irradiation of

SCID mice prior to tumor inoculation has been shown to improve take rates for a number of tumor cell lines (40). Hence, the use of pre-irradiated SCID mice in this study may contribute to a better take rate and enhanced rate of metastases, particularly after co-inoculation with basement membrane Matrigel (36,41). Orthotopic injection of breast cancer cells into the mfps of female mice improves tumor take (36). However, since we only used male mice (which are less costly and easier to obtain), mfp injection was not evaluated. Our results demonstrate that male SCID mice can be used to grow metastatic HER-2-overexpressing breast tumors.

The newly established HCC1954 cell line (17) had not been previously evaluated for *in vivo* growth. We observed that it grew very aggressively after i.p. injection with retained HER-2 expression *in vivo*. This cell line was established from a primary ductal carcinoma and the peritoneal tumors recovered from ascites fluid were organized in large three-dimensional structures with a ductal shape. We found metastases to the lungs in 2 of 5 mice by PCR, however, metastases could not be confirmed by histopathology. Although great care was taken to remove the lungs before opening the peritoneal cavity during autopsy it is possible that the lung tissue was contaminated with HCC1954 cells due to the large tumor burdens. HCC1954 could be a useful model for studying therapies of "ductal" tumors growing in the peritoneum.

MDA-MB-453 has been utilized extensively for *in vitro* studies, but *in vivo* growth has not been reported. This cell line grew relatively poorly *in vivo* and since it also expresses lower levels of HER-2, it is not ideal for studies involving anti-HER-2 MAb therapy.

As has been reported previously using MDA-MB-435 cells (26), the occurrence of

metastases of BT474, HCC1954 and MDA-MB-453 tumor cells to lung, kidney and bone marrow was related to the size of the s.c. tumor and was only detected in mice with the largest s.c. tumors. Although SKOV3.ip1 grew rapidly and formed very large s.c. tumors, we only detected tumor cells in the lung in one of seven mice. However, mice injected with the SKOV3.ip1 cells had to be sacrificed earlier (up to 5 weeks) than the mice with BT474, HCC1954 or MDA-MB-453 tumors due to weight loss and the large size of the tumors. It is possible, therefore, that this was too early for metastatic growth. In tumor models where metastatic development is desirable it may even be advantageous if tumor progression is slow, so that metastases can develop. Furthermore, we observed a fairly large variability in the size of the s.c. tumors in individual mice. It may be necessary to exclude mice with s.c. tumors below a certain size if metastases after surgical removal of the primary tumor are to be studied.

Surprisingly, we did not find any tumor growth in the lungs after i.v. injection of BT474 cells, even though these cells could metasasize to lung after s.c. injection. The reason for this could be that s.c growth is necessary to select for a supopulation of BT474 with metastatic properties which is then capable of growth at other locals. This is supported by the finding that repeated passages *in vivo* can lead to a population with increased metstatic potential.

Shedding of the extracellular portion of HER-2 appears to be common for many HER-2^+ tumors (22,23,42) and sHER-2 has also been detected in sera from cancer patients (23,43-45). The correlation between levels of sHER-2 and tumor burdens may be useful for monitoring tumor development and treatment in general. On the other hand, it is of some concern that the high levels of sHER-2 present in sera may interfere with anti-HER-2 MAb-based tumor therapy since

sHER-2 can neutralize anti-HER-2 MAbs *in vitro* (46). Levels of sHER-2 may decrease, however, by removing the primary tumor prior to treatment of the metastatic lesions, or after chemotherapy.

In the case of lacZ-transfected, MCF-7 breast cancer xenografts (47), removal of the primary subcutaneous (s.c.) resulted in enhanced progression of micrometastases in lymph nodes and bone. Whether lung metastases from s.c. BT474 tumors will also increase after surgical removal of a primary tumor remains to be evaluated.

In conclusion, s.c. injection of the HER-2-overexpressing BT474 cell line leads to routine metastic growth in the lungs where the tumors retain their HER-2 phenotype. This should provide a model for studying HER-2-based immunotherapies to treat MRD after removal of the primary tumor.

Acknowledgements

We thank Dr. Janet Price for the generous gift of BT474, MDA-MB-453 and MDA-MB-435 cells, Dr. Richard Scheuermann and Mr. Greg Hostler for help with the PCR , Dr. Venkatesh Kurvari for helpful advice, Ms. Shannon Flowers for secretarial assistance and Ms. Cindy Self for help with graphics. We also appreciate the expert technical assistance of Ms. Lien Le.

References:

1. Coussens, L., T.L. Yang-Feng, Y.C. Liao, E. Chen, A. Gray, J. McGrath, P.H. Seeburg, T.A. Libermann, J. Schlessinger, and U. Francke. 1985. Tyrosine kinase receptor with extensive homology to EGF receptor shares chromosomal location with neu oncogene. Science **230**: 1132-1139.

2. Slamon, D.J., G.M. Clark, S.G. Wong, W.J. Levin, A. Ullrich, and W.L. McGuire. 1987. Human breast cancer: correlation of relapse and survival with amplification of the HER-2/neu oncogene. Science **235**: 177-182.

3. Di Fiore, P.P., J.H. Pierce, M.H. Kraus, O. Segatto, C.R. King, and S.A. Aaronson. 1987. erbB-2 is a potent oncogene when overexpressed in NIH/3T3 cells. Science **237**: 178-182.

4. Hudziak, R.M., J. Schlessinger, and A. Ullrich. 1987. Increased expression of the putative growth factor receptor $p185^{HER2}$ causes transformation and tumorigenesis of NIH 3T3 cells. Proc.Natl.Acad.Sci.U.S.A **84**: 7159-7163.

5. Révillion, F., J. Bonneterre, and J.P. Peyrat. 1998. ERBB2 oncogene in human breast cancer and its clinical significance. Eur J Cancer **34**: 791-808.

6. Press, M.F., C. Cordon-Cardo, and D.J. Slamon. 1990. Expression of the HER-2/neu proto-oncogene in normal human adult and fetal tissues. Oncogene **5**: 953-962.

7. Disis, M.L. and M.A. Cheever. 1997. HER-2/neu protein: A target for antigen-specific immunotherapy of human cancer. Adv.Cancer Res. **71**: 343-371.

8. King, C.R., P.G. Kasprzyk, P.H. Fischer, R.E. Bird, and N.A. Turner. 1996. Preclinical testing of an anti-*erb* B-2 recombinant toxin. Breast Cancer Res.Treat. **38**: 19-25.

9. Baselga, J., D. Tripathy, J. Mendelsohn, S. Baughman, C.C. Benz, L. Dantis, N.T. Sklarin, A.D. Seidman, C.A. Hudis, J. Moore, P.P. Rosen, T. Twaddell, I.C. Henderson, and L. Norton. 1996. Phase II Study of Weekly Intravenous Recombinant Humanized Anti-

p185^{HER2} Monoclonal Antibody in Patients with HER2/*neu*-Overexpressing Metastatic Breast Cancer. J.Clin.Oncol. **14**: 737-744.

10. Harwerth, I.-M., W. Wels, J. Schlegel, M. Muller, and N.E. Hynes. 1993. Monoclonal antibodies directed to the erbB-2 receptor inhibit in vivo tumour cell growth. Br.J.Cancer **68**: 1140-1145.

11. Pietras, R.J., B.M. Fendly, V.R. Chazin, M.D. Pegram, S.B. Howell, and D.J. Slamon. 1994. Antibody to HER-2/*neu* receptor blocks DNA repair after cisplatin in human breast and ovarian cancer cells. Oncogene **9**: 1829-1838.

12. Ohnishi, Y., H. Nakamura, M. Yoshimura, Y. Tokuda, M. Iwasawa, Y. Ueyama, N. Tamaoki, and K. Shimamura. 1995. Prolonged survival of mice with human gastric cancer treated with an anti-c-erbb-2 monoclonal antibody. Br.J.Cancer **7**: 969-973.

13. King, B.L., D. Carter, H.G. Foellmer, and B.M. Kacinski. 1992. Neu proto-oncogene amplification and expression in ovarian adenocarcinoma cell lines. Am J Pathol **140**: 23-31.

14. Bosma, G.C., M. Fried, R.P. Custer, A. Carroll, D.M. Gibson, and M.J. Bosma. 1988. Evidence of functional lymphocytes in some (leaky) SCID mice. J.Exp.Med. **167**: 1016-1033.

15. Lasfargues, E.Y., W.G. Coutinho, and E.S. Redfield. 1978. Isolation of two human tumor epithelial cell lines from solid breast carcinomas. J.Natl.Cancer Inst. **61**: 967-978.

16. Cailleau, R., R. Young, M. Olive, and W.J. Reeves, Jr. 1974. Breast tumor cell lines from pleural effusions. J.Natl.Cancer Inst. **53**: 661-674.

17. Gazdar, A.F., V. Kurvari, A. Virmani, L. Gollahon, M. Sakagucki, V. Stasny, H.T. Cunmningham, G. Tomlinson, V. Tonk, R. Ashfaq, I.I. Wistuba, J.D. Minna, and J.W. Shay. 1998. Characterization of paired tumor and non-tumor cell lines established from patients with breast cancer. Int.J.Cancer **78**: 766-774.

18. Yu, D., J.K. Wolf, M. Scanlon, J.E. Price, and M.C. Hung. 1993. Enhanced c-erbB-2/neu expression in human ovarian cancer cells correlates with more severe malignancy that can be suppressed by EIA. Cancer Res. **53**: 891-898.

19. Tokuda, Y., Y. Ohnishi, K. Shimamura, M. Iwasawa, M. Yoshimura, Y. Ueyama, N. Tamaoki, T. Tajima, and T. Mitomi. 1996. *In vitro* and *in vivo* anti-tumour effects of a humanised monoclonal antibody against *c-erb*B-2 product. Br.J.Cancer **73**: 1362-1365.

20. Bai, X., G. Hosler, B.B. Rogers, D.B. Dawson, and R.H. Scheuermann. 1997. Quantitative polymerase chain reaction for human herpesvirus diagnosis and measurement of Epstein-Barr virus burden in posttransplant lymphoproliferative disorder. Clinical Chemistry **43**: 1843-1849.

21. Szöllösi, J., M. Balazs, B.G. Feuerstein, C.C. Benz, and F.M. Waldman. 1995. ERBB-2 (*HER2/neu*) gene copy number, $p185^{HER-2}$ overexpression, and intratumor heterogeneity in human breast cancer. Cancer Res. **55**: 5400-5407.

22. Lin, Y.J. and G.M. Clinton. 1991. A soluble protein related to the HER-2 proto-oncogene product is released from human breast carcinoma cells. Oncogene **6**: 639-643.

23. Mori, S., Y. Mori, T. Mukaiyama, Y. Yamada, Y. Sonobe, H. Matsushita, G. Sakamoto, T. Akiyama, M. Ogawa, M. Shiraishi, K. Toyoshima, and T. Yamamoto. 1990. *In vitro* and *in vivo* release of soluble erbB-2 protein from human carcinoma cells. Jpn.J.Cancer Res. **81**: 489-494.

24. Langton, B.C., M.C. Crenshaw, L.A. Chao, S.G. Stuart, R.W. Akita, and J.E. Jackson. 1991. An antigen immunologically related to the external domain of gp185 is shed from nude mouse tumors overexpressing the c-erbB-2 (HER-2/neu) oncogene. Cancer Res. **51**: 2593-2597.

25. Arteaga, C.L., S.D. Hurd, A.R. Winnier, M.D. Johnson, B.M. Fendly, and J.T. Forbes. 1993. Anti-transforming growth factor (TGF)-β antibodies inhibit breast cancer cell tumorigenicity and increase mouse spleen natural killer cell activity. Implications for a possible role of tumor cell/host TGF-β interactions in human breast cancer progression. J.Clin.Invest. **92**: 2569-2576.

26. Price, J.E., A. Polyzos, R.D. Zhang, and L.M. Daniels. 1990. Tumorigenicity and metastasis of human breast carcinoma cell lines in nude mice. Cancer Res. **50**: 717-721.

27. Visonneau, S., A. Cesano, M.H. Torosian, E.J. Miller, and D. Santoli. 1998. Growth characteristics and metastatic properties of human breast cancer xenografts in immunodeficient mice. Am.J.Pathol. **152**: 1299-1311.

28. Ozzello, L. and M. Sordat. 1980. Behavior of tumors produced by transplantation of human mammary cell lines in athymic nude mice. Eur.J.Cancer **16**: 553-559.

29. De Santes, K., D. Slamon, S.K. Anderson, M. Shepard, B. Fendly, D. Maneval, and O. Press. 1992. Radiolabeled antibody targeting of the HER-2/*neu* oncoprotein. Cancer Res. **52**: 1916-1923.

30. Hurwitz, E., I. Stancovski, M. Sela, and Y. Yarden. 1995. Supression and promotion of tumor growth by monoclonal antibodies to ErbB-2 differentially correlate with cellular uptake. Proc.Natl.Acad.Sci.U.S.A **92**: 3353-3357.

31. Yu, D. and M.-C. Hung. 1991. Expression of activated rat neu oncogene is sufficient to induce experimental metastasis in 3T3 cells. Oncogene **6**: 1991-1996.

32. van Slooten, H.-J., B.A. Bonsing, A.J. Hiller, G.T. Colbern, J.H. van Dierendonck, C.J. Cornelisse, and H.S. Smith. 1995. Outgrowth of BT-474 human breast cancer cells in

immune-deficient mice: A new *in vivo* model for hormone-dependent breast cancer. Br.J.Cancer **72**: 22-30.

33. Baselga, J., L. Norton, J. Albanell, Y.-M. Kim, and J. Mendelson. 1998. Recombinant humanized anti-HER2 antibody (herceptin) enhances the antitumor activity of paclitaxel and doxorubicin against HER2/ *neu* overexpressing human breast cancer xenografts. Cancer Res. **58**: 2825-2831.

34. Read, L.D., D. Keith, D.J. Slamon, and B.S. Katzenellenbogen. 1990. Hormonal modulation of HER-2/neu protooncogene messenger ribonucleic acid and p185 protein expression in human breast cancer cell lines. Cancer Res. **50**: 3947-3951.

35. Taverna, D., S. Antoniotti, P. Maggiora, C. Dati, M. De Bortoli, and N.E. Hynes. 1994. erbB-2 expression in estrogen-receptor-positive breast-tumor cells is regulated by growth-modulatory reagents. Int.J.Cancer **56**: 522-528.

36. Price, J.E. 1996. Metastasis from human breast cancer cell lines. Breast Cancer Res.Treat. **39**: 93-102.

37. Mueller, B.M. and R.A. Reisfeld. 1991. Potential of the scid mouse as a host for human tumors. Cancer Metastasis Rev. **10**: 193-200.

38. Xie, X., N. Brünner, G. Jensen, J. Albrectsen, B. Gotthardsen, and J. Rygaard. 1992. Comparative studies between nude and scid mice on the growth and metastatic behavior of xenografted human tumors. Clin.Exp.Metastasis **10**: 201-210.

39. Mitchell, B.S. and U. Schumacher. 1997. Use of immunodeficient mice in metastasis research. British Journal of Biomedical Science **54**: 278-286.

40. Taghian, A., W. Budach, A. Zietman, J. Freeman, D. Gioioso, W. Ruka, and H.D. Suit. 1993. Quantitative comparison between the transplantability of human and murine tumors into the *subcutaneous* tissue of NCr/Sed-*nu/nu* nude and severe combined immunodeficient mice. Cancer Res. **53**: 5012-5017.

41. Mehta, R.R., J.M. Graves, G.D. Hart, A. Shilkaitis, and T.K. Das Gupta. 1993. Growth and metastasis of human breast carcinoma with Matrigel in athymic mice. Breast Cancer Res.Treat. **25**: 65-71.

42. Zabrecky, J.R., T. Lam, S.J. McKenzie, and W. Carney. 1991. The extracellular domain of p185-*neu* is released from the surface of human breast carconoma cells, SK-BR--3. The Journal of Biological Chemistry **266**: 1716-1720.

43. Leitzel, K., Y. Teramoto, E. Sampson, J. Mauceri, B.C. Langton, L. Demers, E. Podczaski, H. Harvey, S. Shambaugh, G. Volas, S. Weaver, and A. Lipton. 1992. Elevated soluble c-erbB-2 antigen levels in the serum and effusions of a proportion of breast cancer patients. J.Clin.Oncol. **10**: 1436-1443.

44. Meden, H., D. Marx, A. Schauer, W. Wuttke, and W. Kuhn. 1997. Prognostic significance of p105 (c-erbB-2, HER2/neu) serum levels in patients with ovarian cancer. Anticancer Res. **17**: 757-760.

45. Krainer, M., T. Brodowicz, R. Zeillinger, C. Wiltschke, M. Seifert, E. Kubista, and C.C. Zienlinski. 1997. Tissue expression and serum levels of HER-2/*neu* in patients with breast cancer. Oncology **54**: 475-481.

46. Brodowicz, T., C. Wiltschke, A.C. Budinsky, M. Krainer, G.G. Steger, and C.C. Zielinski. 1997. Soluble HER-2/neu neutralizes biologic effects of anti-HER-2/neu antibody on breast cancer cells *in vitro*. Int.J.Cancer **73**: 875-879.

47. Kurebayashi, J., M. Nukatsnka, A. Fujioka, S, a, i, t, o, , H, and . 1998. Postsurgical oral administration of uracil and tegafur inhibits progression of micrometastasis of human breast cancer cells in nude mice. Clin.Cancer Res. **3**: 653-659.

48. Liu, Y., D. El-Ashry, D. Chen, I.Y.F. Ding, and F.G. Kern. 1995. MCF-7 breast cancer cells overexpressing transfected *c-erb*B-2 have an *in vitro* growth advantage in estrogen-depleted conditions and reduced estrogen-dependence and tamoxifen- sensitivity *in vivo*. Breast Cancer Res.Treat. **34**: 97-117.

49. Pegram, M.D., R.S. Finn, K. Arzoo, M. Beryt, R.J. Pietras, and D.J. Slamon. 1997. The effect of HER-2/*neu* overexpression on chemotherapeutic drug sensitivity in human breast and ovarian cancer cells. Oncogene **15**: 537-547.

50. Tan, M., J. Yao, and D. Yu. 1997. Overexpression of the c-*erb*B-2 gene enhanced intrinsic metastasis potential in human breast cancer cells without increasing their transformation abilities. Cancer Res. **57**: 1199-1205.

51. Smellie, W.J.B., C.J. Dean, N.P.M. Sacks, M.R. Zalutsky, P.K. Garg, P. Carnochan, and S.A. Eccles. 1995. Radioimmunotherapy of breast cancer xenografts with monoclonal antibody ICR12 against c-*erb*B2 p185: Comparison of iodogen and N-succinimidyl 4-methyl-3-(tri-*n*-butylstannyl) benzoate radioiodination methods. Cancer Res. **55**: 5842s-5846s.

52. Zhang, R.D., I.J. Fidler, and J.E. Price. 1991. Relative malignant potential of human breast carcinoma cell lines established from pleural effusions and a brain metastasis. Invasion Metastasis **11**: 204-215.

Table 1. Tumor take in SCID mice after injection via different routes[1]

Cell Line	Injection Route			
	s.c.		i.p.	i.v.
	+ Matrigel	-Matrigel		
BT474	10/10[2]	7/10	1/10	1/10
HCC1954	9/9	6/9	10/10	N.D.[3]
MDA-MB-453	9/10	7/10	2/5	0/5
SKOV3.ip1	5/5	10/10	3/3	10/10

[1]The tumor cell lines were considered to be successfully xenografted if, at the end of the experiment, the s.c. tumor had a volume >250mm^3, or if macroscopic tumors in tissues were evident, or if tumors were observed by histopathology, or if PCR amplifications of human DNA occurred.

[2]Number of mice with tumor / total number of mice

[3]N.D. = Not Done

Table 2. sHER-2 in culture SNs and sera of tumor-bearing mice

Cell line	sHER-2 in SNs (Units/ml)[1]	sHER-2 in sera from mice injected with tumor cells (Units/ml)[2] via	
		i.p. route	i.v. route
BT474	3400	0	0
HCC1954	2270	75000 +/- 29017	n.d.
MDA-MB-453	937	1040, 780	0
SKOV3. ip1	2590	n.d.	4683 +/- 4045
MDA-MB-435	0	n.d.	n.d.

[1] Cell free culture SNs were collected from confluent cell cultures on day 5.
[2]Sera was collected from 5-9 mice at the time of death (16 weeks for BT474 and MDA-MB-453, 8-11 weeks for HCC1954, 9 weeks for SKOV3.ip1)

Table 3. Published reports describing *in vivo* models of HER-2 overexpressing human breast cancer cell lines

Cell Line	Source/Origin of Tumor	Mouse Strain Used	Injection Route	Metastatic Growth	Reference
MB-3	HER-2 transfectant	Nude	mfp	No	(48)
MCF-7/HER-2		Nude	s.c. + Matrigel	NE[1]	(49)
MDA-MB-435.eB	HER-2 transfectant	SCID	i.v.	Lung	(50)
		SCID	mfp+Matrigel	NE	(50)
MDA-MB-361	Brain metastasis	Nude	s.c.	NE	(51)
		Nude	carotid artery	Brain	(52)
BT474	Primary	Nude	mfp + Matrigel	NE	(36)
		Bg/nu/xid	s.c.+ Matrigel	Lung, lymph node	(32)
		Nude	s.c.	NE	(33)

[1]NE= Not Evaluated

Figure Legends

Figure 1. Mean tumor volume of s.c. tumors after injection with or without Matrigel. 1-2x 10^6 cells, suspended in PBS with (o) or without (•) 50% Matrigel, were injected s.c. into SCID mice. Tumors were measured once a week using calipers. Mean of 8-10 animals ± standard deviation is shown.

Figure 2. Characterization of HCC1954 cells recovered by peritoneal lavage after i.p.injection into SCID mice. (A) HCC1954 cells form ductal shapes during *in vivo* growth. Photographs were taken of HCC1954 cells recovered from the peritoneum 10 weeks after tumor cell inoculation. Magnification 200x (B) HER-2 expression as determined by flow cytometry. Single cell suspensions were prepared from the cells shown in Panel A. Cells were then stained with the anti-HER-2 MAb HER81 (lower panel) or with an isotype-matched, irrelevant control IgG (MOPC-21) (upper panel). Numbers shown in the panels represent % positive cells.

Figure 3. PCR detection of human DNA in mouse lung. Tissues were harvested from a SCID mouse 16 weeks after injection with the human breast cancer cell line BT474 and frozen. DNA was extracted from tissue lysates. PCR reactions included 50-100 ng of DNA and primers which amplified a 300 bp fragment from the human RNApolymerase II gene (Lanes 3-11). GAPDH was amplified as a control (Lanes 12-20). Lane 1= No sample, Lane 2 = DNA size markers, Lane 3 and 12 = No DNA added (negative controls), Lane 4 and 13 = s.c. tumor (positive controls), Lane 5 and 14 = Kidney, Lane 6 and 15 = Lung, Lane 7 and 16 = Spleen, Lane 8 and 17 = Liver, Lane 9 and 18 = Pancreas, Lane 10 and 19 = Testis, Lane 11 and 20 = Bone marrow, Lane 21 and 22 = No sample.

Figure 4. Metastatic growth of tumors as determined by PCR. Mice were sacrificed when moribund or at 16 weeks after tumor inoculation. PCR was performed on DNA purified from frozen tissues as described in the legend to Figure 4. Numbers in parenthesis indicate the number of animals examined. Lung metastases were evident by macroscopic evaluation in mice injected i.v. with SKOV3.ip.1. Only lungs and hearts were examined in mice injected i.p. with HCC1954 cells.

Figure 5. HER-2 expression by metastatic tumor cells in situ. Immunohistochemistry was performed on formalin-fixed, paraffin-embedded lung tissue from mice injected s.c. 16 weeks earlier with BT474 cells. The size of the bar is 200 nm.

Figure 6. Correlation of s.c. tumor size and the levels of sHER-2 in sera. Sera was collected from SCID mice with s.c. tumors larger than 250 mm^3 at the time of death (14-16 weeks after tumor inoculation for BT474, HCC1954 and MDA-MB-453 and 9-11 weeks for SKOV3.ip1). The levels sHER-2 was measured by ELISA as described in Materials and Methods. Each dot represents one mouse. The correlation coefficients for the respective cell lines were; 0.71 for BT474, 0.52 for HCC1954, 0.43 for MDA-MB-453 and 0.59 for SKOV3.ip1.